Synthesis of Heterocyclic [8]Circulenes and Related Structures

Thomas Hensel
Nicolaj N. Andersen
Malene Plesner
Michael Pittelkow*

Department of Chemistry, University of Copenhagen,
Universitetsparken 5, DK-2100 Copenhagen Ø, Denmark
pittel@kiku.dk
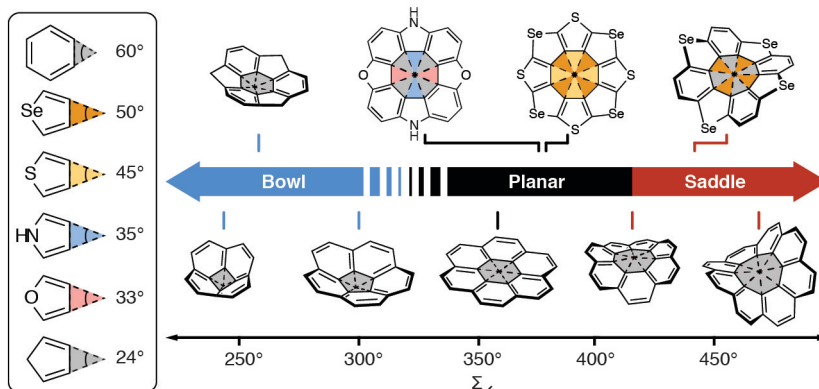
Abstract In this account we give an overview of the synthesis and properties of heterocyclic [8]circulenes. Much of the interest in studying heterocyclic [8]circulenes stems from the planar cyclooctatetraene core often contained in these compounds, which in principle is antiaromatic. We start with a short introduction to the hydrocarbon [n]circulenes and proceed to describe the synthetic chemistry involved in creating tetraoxa[8]circulenes, with particular focus on the acid-mediated oligomerization of benzo- or naphthoquinones, resulting in some simple rules for predicting the outcome of the oligomerization reactions. These rules have guided the synthetic strategies for the preparation of azatrioxa[8]circulenes and diazadioxa[8]circulenes, which will be described in separate sections of this account. More traditional synthetic strategies have been applied in the preparation of octathia[8]circulene, tetrathiatetraselena[8]circulene, and a number of other heterocyclic [8]circulenes, and these synthetic efforts will be highlighted. Finally, a section describing structures that are closely related to the heterocyclic [8]circulenes will be presented, and at the end we will comment on the extensive theoretical work regarding the question of aromaticity/antiaromaticity of the central cyclooctatetraene of heterocyclic[8]circulenes.

1   Introduction

[n]Circulenes (Figure 1) are fully conjugated polycyclic compounds that can formally be derived from the alicyclic [n]radialenes by connecting the termini of the semicyclic double bonds by etheno bridges.[1] Another way to view the [n]circulenes is as a class of compounds that are characterized by having a central ring with [n] sides surrounded by a band of *ortho*-fused benzene rings.

The largest [n]circulene that has been synthesized is [8]circulene (**6**) as a π-extended derivative, and the largest [n]circulene that has been described computationally is [20]circulene.[1a] As [3]radialene is known, one might expect that [3]circulene would exist as well, but so far the synthesized [n]circulenes only span the bowl-shaped [4]circulene **2** and [5]circulene **3**, the planar [6]circulene **4** and the saddle-shaped [7]circulene **5** and [8]circulene **6** (Figure 1). In a computational study, Hopf and co-workers predicted the geometries of all hydrocarbon [n]circulenes from the [3]circulene **1** to [20]circulene.[1a] They described the strain energy associated with enlarging the [n]circulene structure as compared to the energy associated with [6]circulene **4**. The larger structures become helical, as predicted by density functional theory (DFT) calculations. The existence of a [3]circulene is considered unfeasible.

Heterocyclic circulenes are [n]circulenes where one or more of the etheno bridge(s) have been replaced with a heteroatom such as oxygen, sulfur, nitrogen, or selenium. Some of the known hetero[8]circulenes (substituents not shown) are presented in Figure 2. The slightly different geometries of furan, thiophene, pyrrole, and other five-membered 6π-aromatic systems as compared to benzene make the heterocyclic [8]circulenes very different from hydrocarbon [8]circulenes, both in their geometry and chemical and physical properties. The relationship between the structures of circulenes and the geometries of these compounds

has attracted significant interest.[1] The emergence of non-planar, fully conjugated systems, such as the fullerenes and carbon nanotubes, has certainly served as an inspiration for studies of the fundamental properties of non-planar circulenes.[2] In an early study, Dopper and Wynberg introduced a simple yet efficient approach for analyzing the geometry of circulenes using a mathematical model containing the inner (r_1) and outer (r_2) radii of the circulene, and the length of the spokes (a).[3] From this model, it is possible to assess quickly, without the need of computational modelling,

whether the circulene is planar or bowl-shaped as shown in Figure 3. We believe that Dopper and Wynberg's model falls short in its ability to predict saddle-shaped circulenes, as it can be difficult to define an outer radius of a saddle. We therefore propose an alternative model in which the wedge angles of the aromatic moieties are summed, as shown in Figure 4. This model was inspired by considerations from Högberg's doctoral thesis.[4] The wedge angles are derived from literature DFT calculations[5] using the C–C–C bonding angle of the cyclic compounds. Comparing the sum of the

Biographical Sketches

Thomas Hensel received his M.Sc. degree from Leipzig University in 2012. Supported by the Erasmus program, the practical work of the master's degree was carried out in Michael Pittelkow's group at the University of Copenhagen. He is currently a Ph.D. student under the direction of Michael Pittelkow at the Department of Chemistry, University of Copenhagen, working on the synthesis and applications of novel hetero-[8]circulenes.

Nicolaj Nylandsted Andersen was born in 1991 on the island of Funen, Denmark. He completed his B.Sc. in 2013 and his M.Sc. in 2015 at the Department of Chemistry, University of Copenhagen under the supervision of Michael Pittelkow. During his bachelor's and master's studies, he has been developing helicene chemistry with possible applications in DNA recognition. He is currently pursuing a Ph.D., working with bio-tin[6]urils, again under the supervision of Michael Pittelkow. He was a recipient of the Novo Scholarship Programme in 2014.

Malene Plesner was born in Copenhagen in 1989. She studied chemistry at the University of Copenhagen and received her B.Sc. degree in 2012 under the supervision of Professor John Nielsen. In 2014, she completed her M.Sc. degree supervised by Michael Pittelkow within the field of synthetic organic chemistry, focusing on the synthesis and characterization of different azatrioxa[8]circulenes. She is currently teaching high school chemistry at Johannesskolen, Copenhagen.

Michael Pittelkow was born in Brøndby Strand, near Copenhagen. He studied chemistry at the University of Copenhagen where he received his Ph.D. degree in 2006 under the supervision of Associate Professor Jørn B. Christensen. During his studies he spent extended periods in Australia (CSIRO in Melbourne, with Dr. Kevin Winzenberg), The Netherlands (The Technical University of Eindhoven, with Professor E. W. Meijer) and the U.K. (University of Cambridge). He undertook postdoctoral training at the University of Cambridge under the mentorship of Professor Jeremy K. M. Sanders before moving back to the University of Copenhagen. In 2013, he became an associate professor. His research interests include organic synthesis, physical organic chemistry, dynamic combinatorial chemistry and supramolecular chemistry.

wedge angles, $\Sigma_{\angle}$, one intuitively expects circulenes with $\Sigma_{\angle}$ values close to 360° to be planar, whereas lower $\Sigma_{\angle}$ indicate bowls and higher $\Sigma_{\angle}$ saddles.

Figure 1 Structures of [n]circulenes. (a) [n]Circulenes may be viewed as derivatives of [n]radialenes or as rings of *ortho*-fused benzene rings. (b) Geometries of [n]circulenes
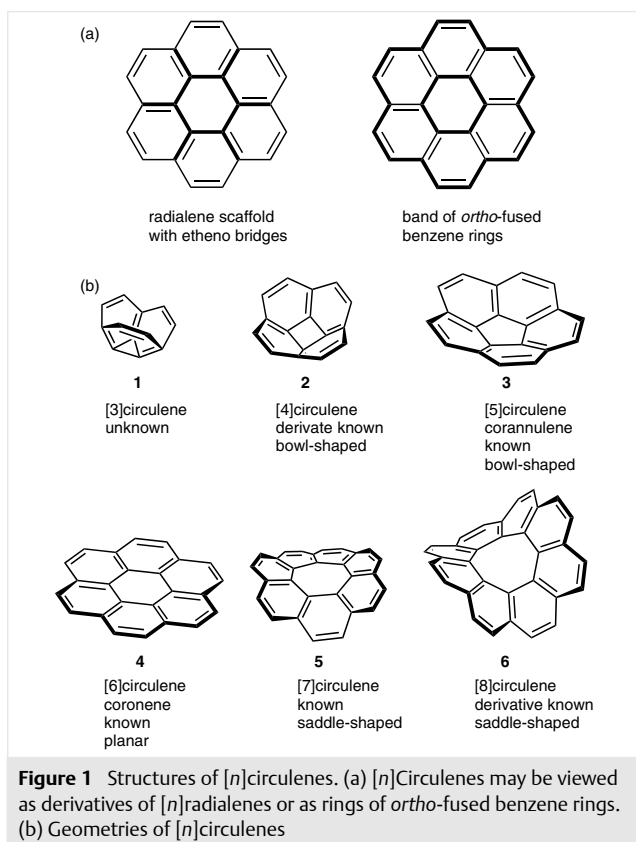
By comparing 15 circulenes,[3,6] we found that planar circulenes indeed reside in a narrow interval between 336° and 380°. An exception is tetrathia[8]circulene **9** at 420°. The bond angles of the thiophene moieties of this circulene deviate significantly from those found in thiophene itself, indicating that the elasticity of the thiophene moiety facilitates the formation of a planar heterocyclic [8]circulene. The transition to the helical geometry discussed computationally by Hopf occurred at $\Sigma_{\angle}$ around 1000°, with a transition from saddle-shaped [16]circulene ($\Sigma_{\angle}$ 960°) to helical [17]circulene ($\Sigma_{\angle}$ 1020°).[1a] The lack of compounds does, however, make this geometry speculative for now, and synthesizing the strained helical structures will surely be a challenge. We are looking forward to seeing new circulenes being synthesized and characterized structurally to further validate our model. We especially welcome entries which can fill the gap between [5]- and [6]circulene so that the limit of $\Sigma_{\angle}$ between bowl-shaped and planar circulenes can be determined more precisely. In this account we will briefly describe the seminal work on the syntheses of all-hydrocarbon [n]circulenes as well as a more comprehensive de-

Figure 2 Structures of synthetically available heterocyclic [8]circulenes. The core structures are shown without substituents
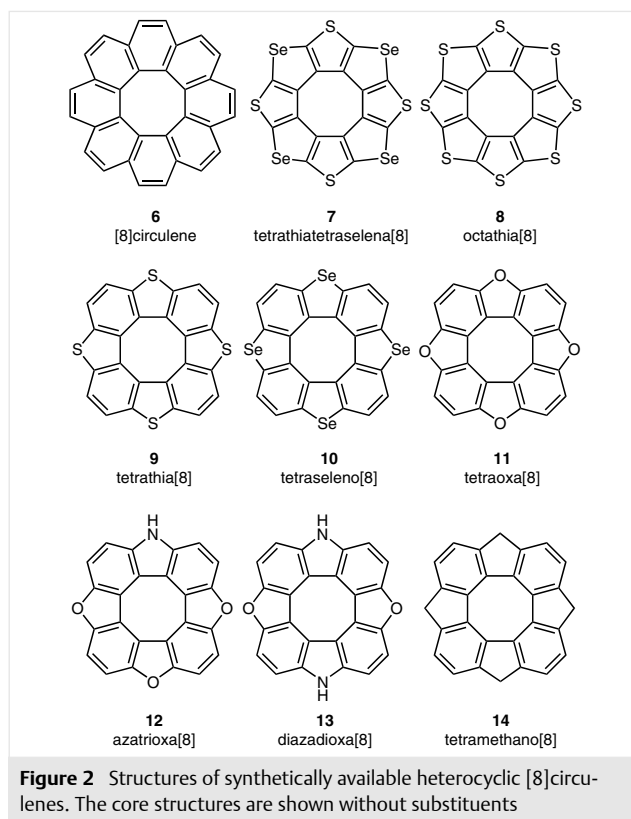
scription of the synthetic work developed for the syntheses of heterocyclic [8]circulenes. We will devote special emphasis on the early work developed by Erdtman and Högberg on the preparation of tetraoxa[8]circulenes and how the mindset developed in their work has inspired our syntheses of azatrioxa- and diazadioxa[8]circulenes. We will also describe the synthetic efforts in developing other types of heterocyclic [8]circulenes ranging from the parent octathia[8]circulene **8** to tetraaza[8]circulenes embedded in large π-extended porphyrin arrays. Finally, we will focus on a range of compounds that are related to heterocyclic [8]circulenes, in that they contain a planar cyclooctatetraene (COT) structure, and we will discuss the antiaromatic character of this moiety.

Figure 3 Dopper and Wynberg's model. The geometry is estimated using the inner radius (r_1), outer radius (r_2), and length of the spokes (a)
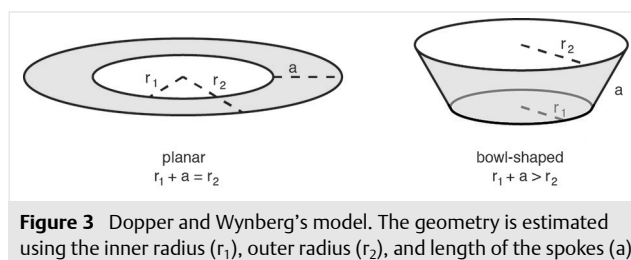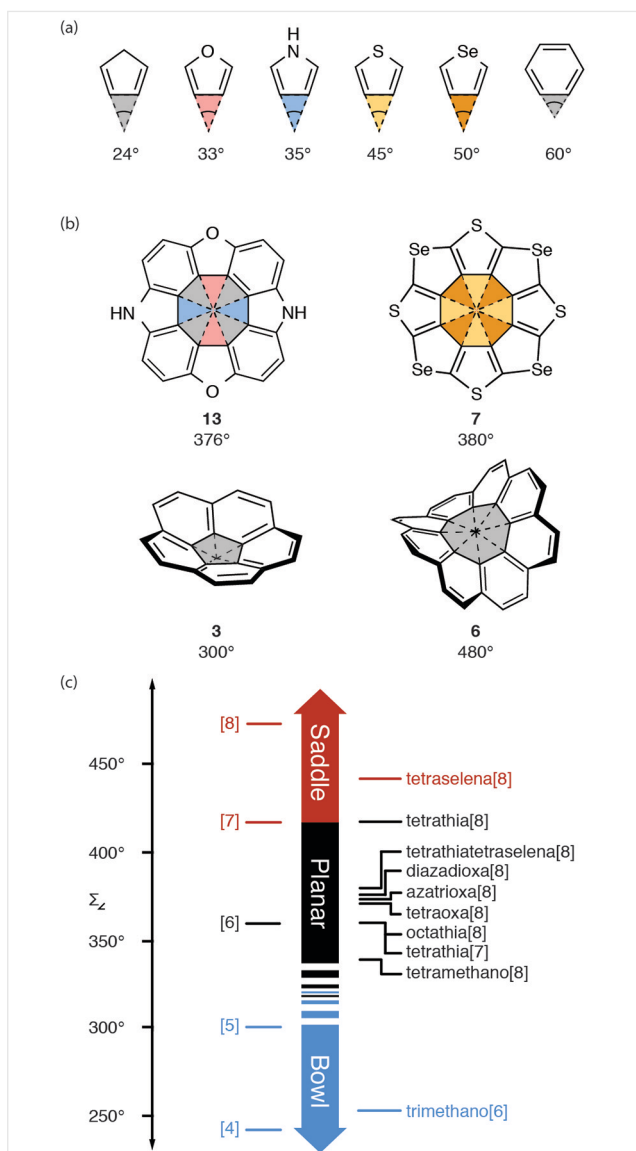
Figure 4 A model for estimating the geometry of circulenes based on heterocyclic moieties. (a) Wedge angles of common aromatic rings and cyclopentadiene. (b) Visual interpretation of circulene geometry using the wedge angles to form $\Sigma_\angle$. (c) Spectrum of $\Sigma_\angle$ values of known circulenes and their corresponding geometries. The circulene suffix has been omitted for clarity

2 Synthesis of [n]Circulenes

The crystal structures of [4]- to [8]circulenes are depicted in Figure 5. Only [5]-, [6]-, and [7]circulene have been synthesized without substituents.

2.1 [4]Circulene

[4]Circulene **2** (quadrannulene) is, to date, the smallest [n]circulene, and was prepared as a π-extended derivative by King and co-workers in 2010.[6e,7]
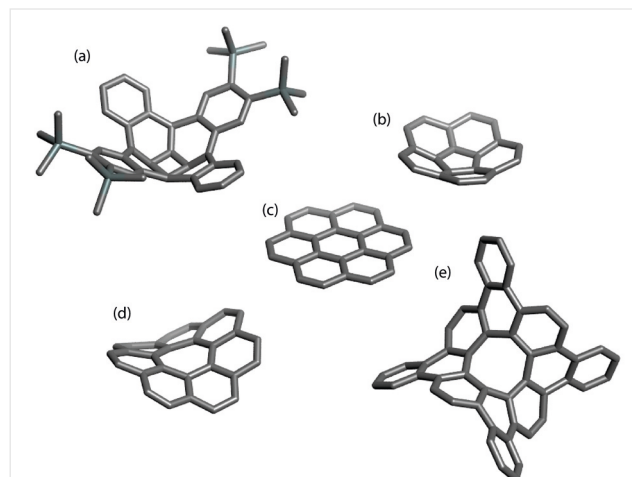
Figure 5 X-ray crystal structures of [n]circulenes. (a) A [4]circulene derivative. (b) [5]Circulene. (c) [6]Circulene. (d) [7]Circulene. (e) An [8]circulene derivative. (X-ray crystal data are from the Cambridge Structural Database)

Hopf and co-workers have outlined different possible synthetic strategies toward the preparation of [4]circulenes.[1a] The King group used one of the Hopf strategies in their synthesis of a π-extended [4]circulene derivative (**18**).[7] Although the yield of the synthesis reported was not impressive, the elegance of the synthetic route was remarkable. The [4]circulene **18** is obtained in only five steps via a final cobalt-mediated cyclotrimerization (Scheme 1).
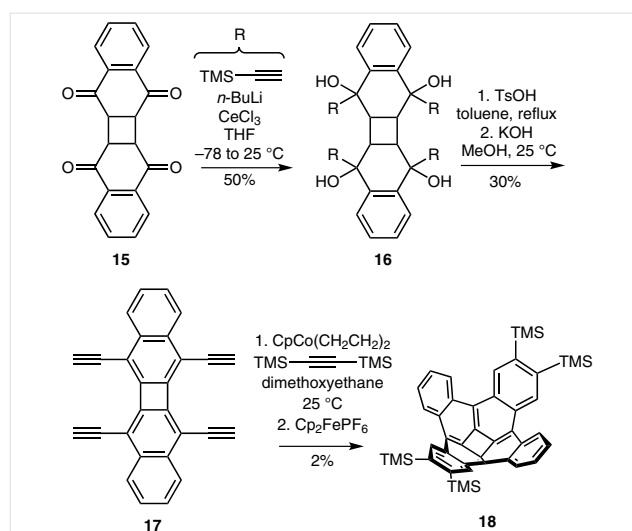
Scheme 1 Synthesis of a quadrannulene derivative by King and co-workers

The crystal structure of the [4]circulene **18** supported the bowl predicted by Hopf. Though [4]- and [5]circulene are both bowl-shaped, the bowl inversion barrier of the two are quite different, with [4]circulene being at a staggering 120 kcal mol^{-1} compared to that of [5]circulene at 9 kcal mol^{-1}, thereby showing the rigid nature of the product.[1a]

2.2 [5]Circulene

[5]Circulene **3** (corannulene) is the second lowest [n]circulene. The synthesis of [5]circulene was first reported by Barth and Lawton in 1966.[8] Their strategy was to build the [5]circulene one ring at a time starting from an ester-substituted phenanthrene (Scheme 2a). In the final step, an aromatization over palladium-on-carbon gave the corannulene. The amount of steps in this synthesis was overwhelming. In 1991, a more viable synthesis using a different approach was reported by Scott et al.[6j] Their approach was to use flash vacuum pyrolysis to form [5]circulene directly from a substituted flouranthene **21** (Scheme 2b).

Extensive research on the synthesis and properties of corannulene and several synthetic procedures have since been reported.[9] Much of the work appears to have been driven by the fact that [5]circulene may be viewed as a fragment of the spherical C_{60} molecule. The bowl-shape of [5]circulene and its resemblance to the fullerenes also makes it an attractive starting point for the synthesis of larger fragments of the fullerenes and even for the synthesis of carbon nanotubes.[6j]

Scheme 2 Synthesis of corannulene. (a) First reported synthesis by Barth and Lawton. (b) Flash vacuum pyrolysis approach reported by Scott et al.
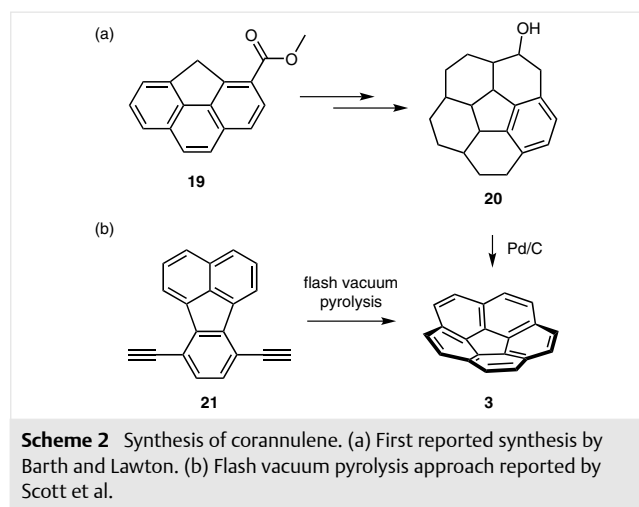
2.3 [6]Circulene

[6]Circulene **4** (coronene) was the first hydrocarbon circulene to be synthesized.[10] While [5]circulene may be viewed as a fragment of the fullerenes, [6]circulene may be regarded as being a fragment of graphene.[11]

The final steps of the synthesis by Scholl and Meyer can be seen in Scheme 3a.[10] In their approach, the dibenzocoronene **22** was synthesized followed by oxidation with nitric acid to give first the dibenzocoronene quinone **23** and then the coronene tetracarboxylic acid **24**. In the final step, the coronene tetracarboxylic acid **24** was heated to 500 °C in the presence of calcium hydroxide to give the coronene **4**. Other approaches for the synthesis of [6]circulene have been developed including one utilizing a ruthenium-catalyzed benzannulation (Scheme 3b).[12] The high stability of coronene is reflected by the fact that it exists in Nature as the mineral carpathite.[13]

Scheme 3 Synthesis of [6]circulene. (a) First reported synthesis by Scholl and Meyer. (b) Ruthenium-catalyzed benzannulation reported by Shen et al.
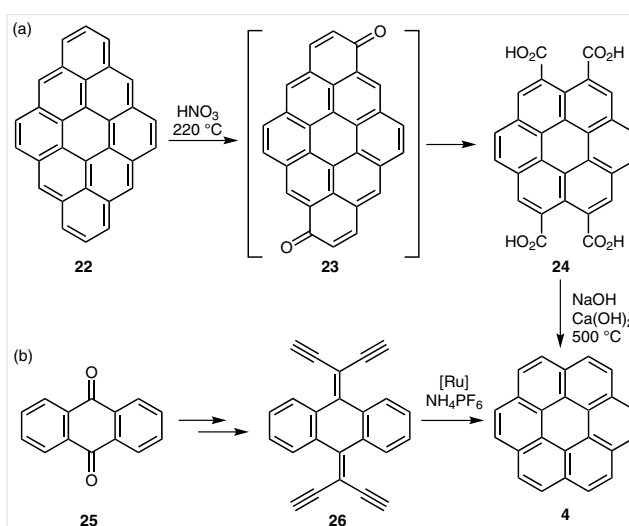
2.4 [7]Circulene

[7]Circulene **5** (pleiadannulene) is saddle-shaped and was first synthesized in 1983 by Yamamoto et al.[6k] Their synthetic approach was to first close the central seven-membered ring followed by the formation of the final benzene ring to complete the [7]circulene (Scheme 4a). The [7]circulene was crystallized, from which the saddle-shaped geometry was confirmed.[14] In 1996, a different synthetic method was described.[15] Here the formation of both the central ring and the peripheral ring was accomplished in a single step using flash vacuum pyrolysis. Finally, the saturated positions were dehydrogenated using palladium-on-carbon to give the fully unsaturated [7]circulene (Scheme 4b).

2.5 [8]Circulene

The syntheses of [8]circulene derivatives have very recently been reported by three different groups.[6d,16] The strain inherent to the [8]circulene has been a possible hin-

T. Hensel et al.

Scheme 4 Synthesis of [7]circulene. (a) First reported synthesis by Yamamoto et al. (b) Flash vacuum pyrolysis approach

Scheme 5 Synthesis of [8]circulene derivatives. (a) Using a palladium-catalyzed cross-coupling approach. (b) Using a Diels–Alder reaction and a palladium-catalyzed cross-coupling approach
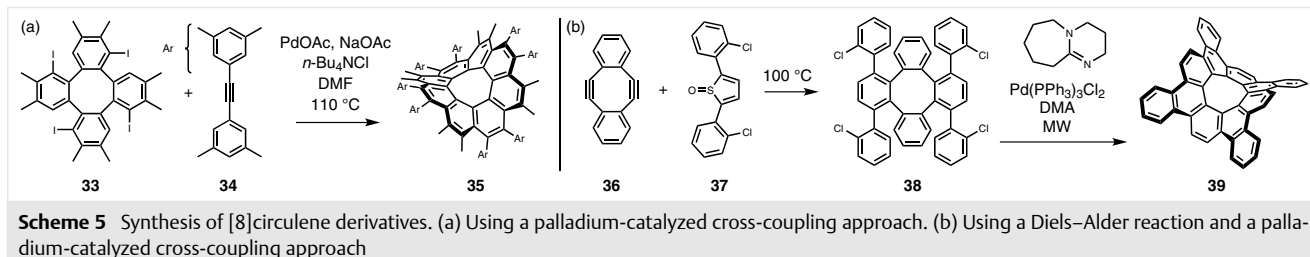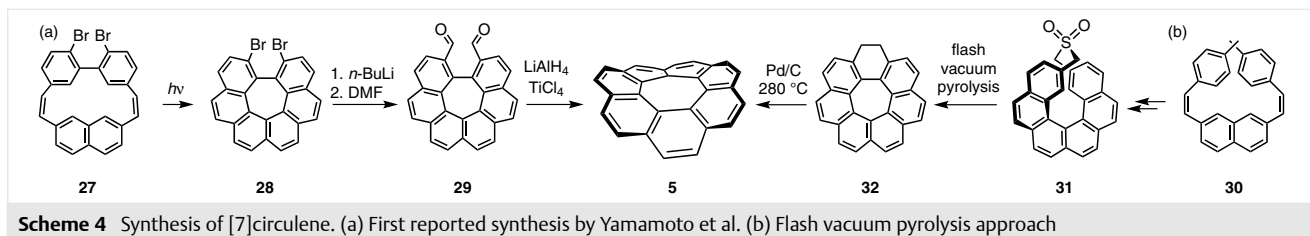
drance for the synthesis of this particular [*n*]circulene. The first reported synthesis uses palladium-catalyzed annulations to give the [8]circulene derivative **35** in a single step (Scheme 5a).[6d] The second combines two molecules by a Diels–Alder reaction. Subsequently, the intermediate **38** is closed using a palladium-catalyzed cross-coupling to yield the [8]circulene derivative **39** (Scheme 5b).[16a]

3 Synthesis of Tetraoxa[8]circulenes: A Historical Perspective

Tetraoxa[8]circulenes **11** can be prepared from 1,4-benzoquinones in yields that depend on the substitution pattern of the 1,4-benzoquinone (Scheme 6). Dihydroxydibenzofuran (**40**) was found to be an important intermediate in the transformation.[17]

Scheme 6 Retrosynthetic analysis of tetraoxa[8]circulene
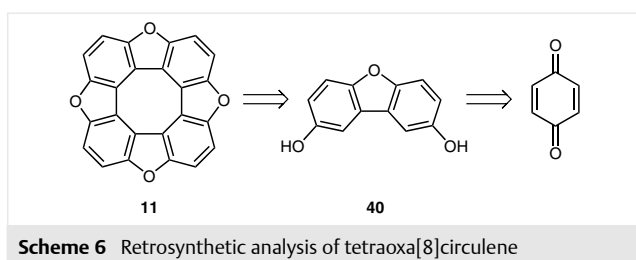
It was first observed by von Knapp and Schultz[18] in 1881, and Liebermann[19] in 1885, that mixing 1,4-naphthoquinones under acidic conditions led to an insoluble oligomerization product. The work connecting the discoveries of the 19th century with modern day tetraoxa[8]circulene chemistry is outlined in this section. Erdtman described his work on quinone reactivity in a series of publications in 1933.[20] The reactivity and stability of substituted benzoquinones were examined with the foundation of the work being the high stability of unsubstituted 1,4-benzoquinone

compared to substituted derivatives.[20a] This was attributed to the competition of mesomeric polarization on the quinoid core by the two carbonyl groups: the core had a diffuse cationic character, and as such was not prone to regiospecific nucleophilic attack. 2-Methoxy-1,4-benzoquinone (**41**) acted differently: the symmetry of this system had been disrupted, and the carbonyl group at the position 4 now had its electron demand satisfied by donation from the methoxy substituent. This makes the 5,6 double bond polarized, mainly due to the carbonyl group at position 1, leading to reaction in a Michael fashion in the Thiele acetylation (Scheme 7). The scheme also depicts the reaction product of 2-methoxy-5-methyl-1,4-benzoquinone (**43**). The reactive 5-position had been blocked, but having the same carbonyl group dictate reactivity, the reaction occurs at position 3, although slower than in the former example.

Scheme 7 Regioselectivity of the Thiele acetylation of benzoquinones as discussed by Erdtman. The positions discussed in the text have been numbered
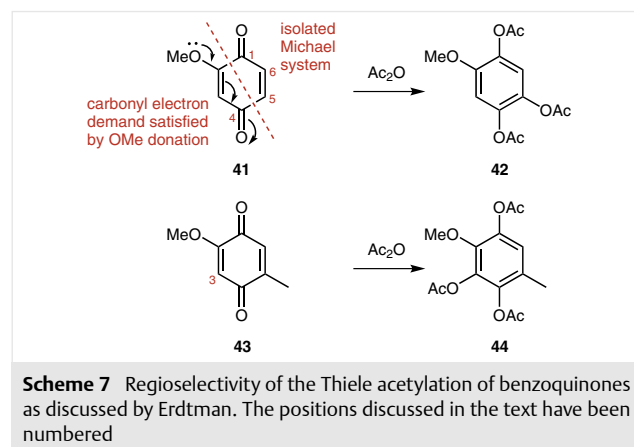
In addition to the two-electron mechanisms described above, radical coupling of quinones was also investigated by Erdtman:[20b] the possibility of isomerization between oxygen and carbon radicals for phenols was discussed based on literature reports by Pummerer, with prediction of reactivi-

ty at *ortho*- and *para*-positions.[21] In the oxidative coupling of benzoquinone, the regioselectivity was predicted based on the Michael addition model and confirmed experimentally. The reactivities of 2-substituted benzoquinones followed the same trend as for Thiele acetylation: HO > MeO > Me > H (Scheme 8). The subsequent formation of furan rings was analyzed[20c,d] with the proposed mechanism depicted in Scheme 9. The same trend in reactivity as for the benzoquinone couplings was observed. For 2-methyl-1,4-benzoquinone, a product of condensation 48 was observed that contained two phenolic and two furanic oxygen atoms. It was suggested that the reduced reactivity of the methyl derivative facilitates new reaction pathways to yield a termolecular product, with the proposed structure shown in Figure 6. The formation of the furan rings from 2-methyl-1,4-benzoquinone had to occur with nucleophilic attack on the carbonyl groups in order to arrive at the proposed structure. Also depicted in Figure 6 is the proposed structure of the product of condensation of naphthoquinone, the tribenzotrioxa[6]circulene 49. This trimeric structure was retracted and the tetrameric structure 50 was proposed based on mass spectrometry in a publication from 1968.[22] Disregarding the incorrect structure elucidation, this was nevertheless the first report of a tetraoxa[8]circulene.
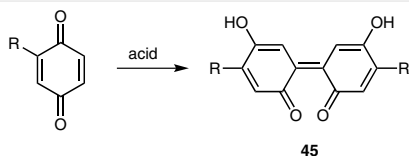
Scheme 8 Reactivity of benzoquinones in a dimerization reaction. R: OH, OMe, Me, or H
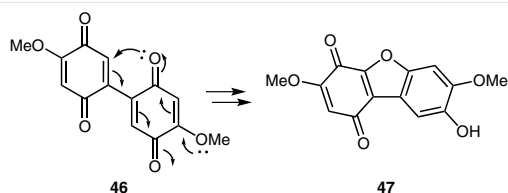
Scheme 9 Formation of furan rings as investigated by Erdtman
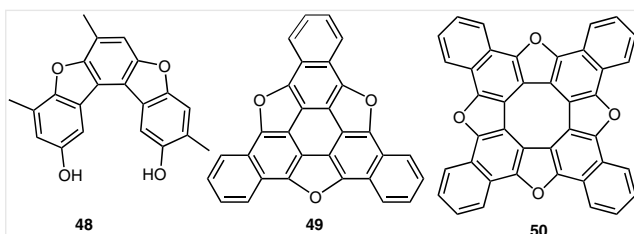
Figure 6 Structures from the work of Erdtman. Compound 48: structure of the product obtained from condensation of 2-methyl-1,4-benzoquinone. Compound 49: proposed structure of the product of the condensation of naphthoquinone. Compound 50: corrected structure of the tetrameric condensation product
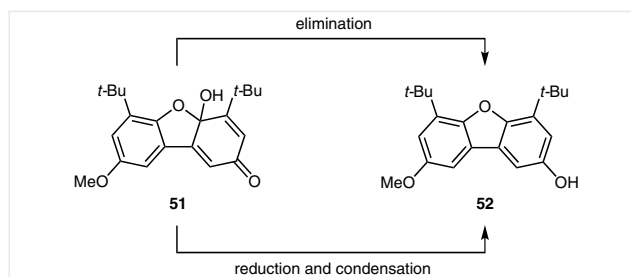
Scheme 10 Overview of the synthetic structure elucidation performed by Hewgill and Kennedy
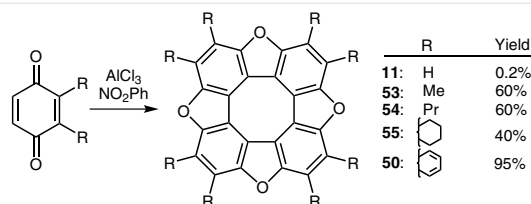
Scheme 11 Formation of tetraoxa[8]circulene from 2,3-disubstituted 1,4-benzoquinones. Increasing 2,3-disubstitution increases the yield of the reaction

In 1966, Hewgill and Kennedy further examined intermediates in the formation of dibenzofurans from benzoquinones.[23] The structure of the intermediate hemiacetal 51 was confirmed both with NMR spectroscopy and by two transformations converging at the monohydroxy compound 52, as shown in Scheme 10.

Erdtman and Högberg reported on a whole series of tetraoxa[8]circulenes in 1970.[24] 2,3-Disubstitution at the 1,4-benzoquinone led to increased yields (Scheme 11), and the authors stated that the circulenes might be formed by two competing pathways, that is, by sequential addition of monomers or by combination of two dimers.

Following his collaboration with Erdtman, Högberg released a series of papers entitled '*Cyclo-oligomerizations of Quinones*', beginning in 1972.[17,24b,25] He noticed that adding dihydroxydibenzofuran 40 increased the yield of tetraoxa[8]circulene, further indicating that this was indeed an intermediate of the reactions. In addition, a conclusion was reached that 2,3-disubstitution was favored over 2-monosubstitution in the formation of circulenes, in accordance with the quinone couplings seen by Erdtman in 1933. Högberg also showed that it was possible to create mixed dimers, trimers and circulenes from resorcinol, naphthoquinone, and benzoquinone. The resorcinol acted as a terminator, preventing further oligomerization due to the lack of *ortho* or *para* relationships between substituents.

In 1977, Erdtman joined Högberg again, collaborating on providing crystal structures of the dihydroxydibenzofuran 40 and the trimer and open tetramer of benzoquinone,[26] giving some concluding remarks on the mechanistic aspect of the formation of circulenes.[27] They observed that adding a strong oxidant, chloranil, inhibited the reaction,
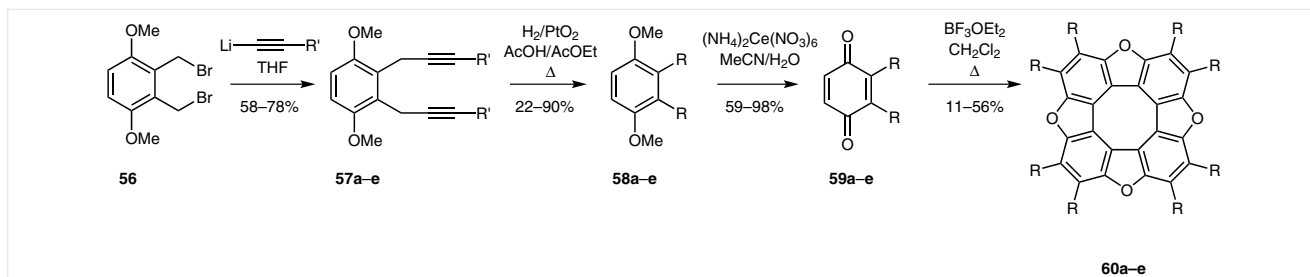
Scheme 12 Synthesis of octaalkylated tetraoxa[8]circulenes. R′ = *n*-butyl to *n*-octyl. R = *n*-heptyl to *n*-undecyl

indicating that hydroquinone was needed for the reaction to proceed, and suggesting a hemiketal intermediate in the reaction and a non-radical mechanism.

Some of the first well-soluble tetraoxa[8]circulenes, synthesized with liquid crystallinity in mind, were described by Christensen and co-workers in 2000.[28] Alkyl chains of different length (C_7 to C_{11}) on the benzene moieties were achieved by reaction with an alkynyllithium compound on a bis-bromomethyl compound **56**, followed by reduction of the triple bond with hydrogen/platinum(IV) oxide (H_2/PtO_2), yielding 2,3-dialkyl-1,4-dimethoxybenzenes **58a–e** (Scheme 12). After oxidation with cerium(IV) ammonium nitrate,[29] the 2,3-dialkyl-1,4-benzoquinones **59a–e** were reacted with boron trifluoride–diethyl ether complex (BF₃·OEt₂) in boiling dichloromethane to give differently alkylated tetraoxa[8]circulenes **60a–e**.

There were two distinct phase transitions observed in the substances with heptyl, octyl, nonyl or decyl chains, with increasing chain length lowering both the transition temperatures. These compounds also showed other physical properties associated with liquid crystallinity, such as birefringence (dependence of the refractive index on the polarization and direction of propagation of light) and shearability (deformation of the liquid crystal after applying a unidirectional force). This was in contrast to an octapropyl derivative (prepared from 2,3-dipropylbenzoquinone), which did not show liquid crystallinity.[28]

Efforts by Rathore and co-workers resulted in bicyclo[2.2.2]octane- and bicyclo[2.2.1]heptane-annulated tetraoxa[8]circulene derivatives.[30] The synthetic pathway leading to compounds **65a** and **65b** is depicted in Scheme 13.

Both [8]circulenes were submitted to optical and electrochemical spectroscopy and were oxidized to form stable radical-cation salts.

In 2010, Christensen and Pittelkow constructed organic light-emitting diodes (OLEDs) using tetraoxa[8]circulenes.[31] The compounds discussed in their paper (**50** and **66**–**70**) were produced in a statistical condensation of 1,4-naphthoquinone and 2,3-undecyl-1,4-benzoquinone with boron trifluoride–diethyl ether complex in boiling dichloromethane (Scheme 14). A tetraundecyldinaphthocirculene with *trans*-configuration of the substituents was found to have a quantum yield of 0.83, and the octaundecylcirculene was found to emit blue light, which is valuable in the development of OLEDs.

In another publication by our group, the unusual aggregation behavior of different regioisomers of tetra-*tert*-butyltetraoxa[8]circulene **71**–**74** was examined (Scheme 15).[32] A condensation reaction of four 2-*tert*-butyl-1,4-benzoquinones with boron trifluoride–diethyl ether complex in dichloromethane yielded all four regioisomers. The compounds were highly soluble in dichloromethane and heptane.

The four-fold symmetrical tetraoxa[8]circulene **71** was isolated from the mixture by dry column flash chromatography, and product **72** was crystallized from the remaining mixture. Figure 7 depicts the herringbone crystal packing of **71**.

The reaction of **71** with aluminum chloride (AlCl₃) in boiling benzene enabled us to produce the insoluble tetraoxa[8]circulene **11** in quantitative yield (Scheme 16). A recent member of the tetraoxa[8]circulene family was syn-
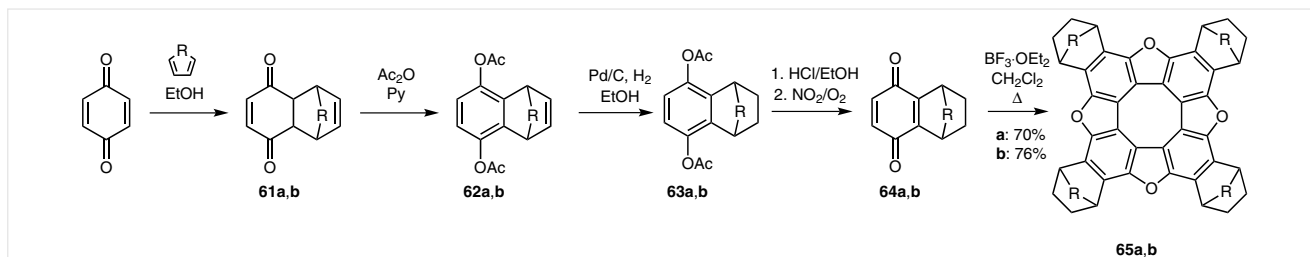
Scheme 13 Synthesis of bicyclo-annulated tetraoxa[8]circulenes. **a**: R = –CH₂–; **b**: R = –CH₂CH₂–
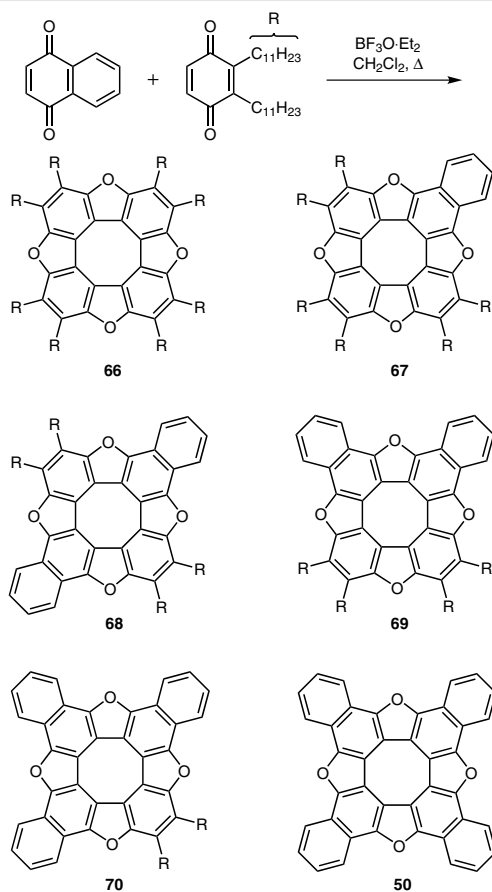
Scheme 14 Condensations of 1,4-quinones. The product mixture is composed of all the possible regioisomers
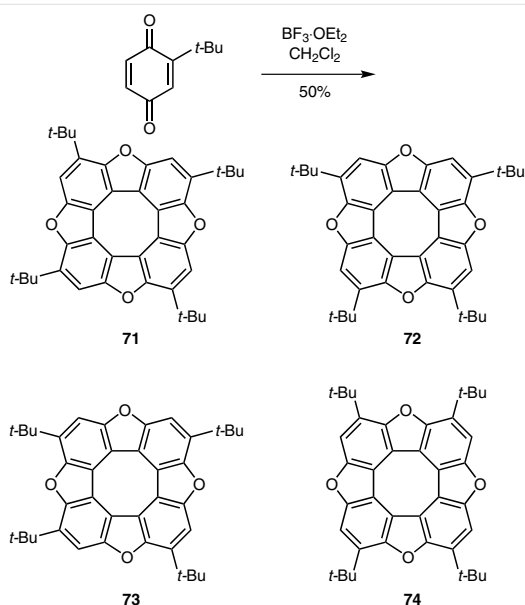
Figure 7 X-ray crystal structure of regioisomer **71**

thesized in 2014 by Christensen.[6a] The geminally dialkylated tetraindanotetraoxa[8]circulene **82** was devised and synthesized with a possible application as a discotic liquid crystal system in mind. The synthetic pathway had 2,5-dimethoxybenzaldehyde (**75**) as a starting material, yielding 4,7-dimethoxy-2,3-dihydro-1*H*-inden-1-one (**81**) after six steps. Condensation using boron trifluoride–diethyl ether complex in dichloromethane gave the tetraoxa[8]circulene **82** (Scheme 17). However, the product did not show any mesophase by differential scanning calorimetry (DSC).
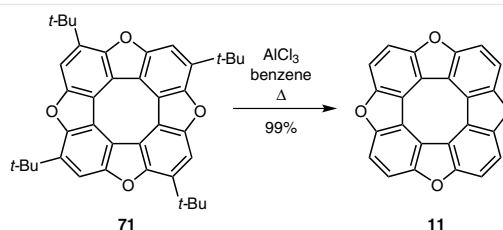
Scheme 16 De-*tert*-butylation producing the unsubstituted tetraoxa[8]circulene **11**

4 Synthesis of Azatrioxa[8]circulenes

The previous section addressed Högberg's and Erdtman's work on the acid-mediated condensations of 1,4-benzo- and 1,4-naphthoquinones. They observed different linear phenolic and furanic structures and concluded that 3,6-dihydroxydibenzofuran was an important intermediate (Scheme 6).[27] Derived from these results, we set out to synthesize azatrioxa[8]circulenes using dihydroxycarbazole as an analogue of dihydroxydibenzofuran (Scheme 18). A few challenges arose from using 9*H*-carbazole: both positions α to the hydroxy groups are reactive toward coupling with 1,4-benzoquinone. The resulting non-regioselective oxidative coupling would yield regioisomers. Allowing only reactivity at the 4- and 5-positions required blocking the 2- and 7-positions, preferably using bulky protecting groups that would also increase the solubility of the compounds by preventing aggregation between the large π-systems. In the

Scheme 15 Synthesis of tetra-*tert*-butyltetraoxa[8]circulenes **71–74**

Scheme 17 Synthesis of a geminally dialkylated tetraindanotetra-oxa[8]circulene **82**

Scheme 18 Retrosyntheses of tetraoxa[8]circulene **83** and azatri-oxa[8]circulene **85**. Numbering of the carbazole positions is shown
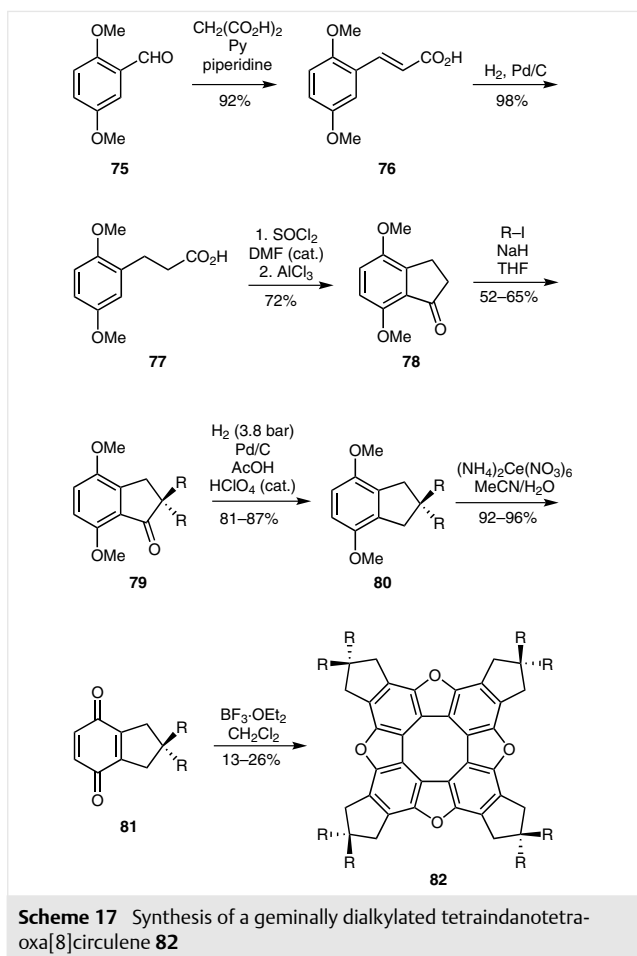
work with tetraoxa[8]circulenes, we had previously shown that *tert*-butyl groups were desirable for guiding the reactivity and achieving high solubility in organic solvents. Another reactive center, the carbazole nitrogen, needed protection from undesired reactions. On the basis of these requirements, the formation of azatrioxa[8]circulenes from reactions of a suitably substituted 3,6-dihydroxy-9*H*-carbazole with 1,4-benzoquinones or 1,4-naphthoquinone was investigated. The presence of *tert*-butyl groups at the 2- and 7-positions prevented polymerization, driving the reaction toward the cyclic product. A benzyl group was chosen for the protection of the nitrogen at the 9-position based on its stability and many means of deprotection. Different alkyl chains were also employed for blocking the nitrogen. It was important to utilize a 1,4-quinone with substituents at either the 2-position or both the 2- and 3-positions in order to avoid unwanted condensation products, as experienced by Erdtman and Högberg.[4,17,22,24–27] The synthetic pathway starting from 9*H*-carbazole yielding *N*-substituted 2,7-di-*tert*-butyl-3,6-dihydroxycarbazoles **91** and **92** is presented in Scheme 19.[6b] The 9*H*-carbazole was protected with a benzyl or propyl group by phase-transfer catalysis. *N*-Ben-

zyl- or *N*-propylcarbazole was then brominated at the 3- and 6-positions. In the subsequent step, the dibromo compounds **88a,b** were transformed into dimethoxycarbazoles **89a,b**, which underwent Friedel–Crafts *tert*-butylation to block the 2- and 7-positions, thereby increasing the solubilities of the products. The *N*-propyl-2,7-di-*tert*-butyl-3,6-dimethoxycarbazole **90a** was demethylated with boron tribromide (BBr$_3$) in dichloromethane.[33] Boron tribromide proved inefficient in the demethylation of *N*-benzylcarbazole **90b**, as the benzyl group was also cleaved resulting in an oxidation-sensitive compound. Increased reaction times for the demethylation led to cleavage of the *tert*-butyl groups. Various attempts using, for example, AlCl$_3$, lithium iodide (LiI), sodium 1-butanethiolate (NaSBu) or sodium benzeneselenolate (PhSeNa) did not yield the desired product **92**. Only adding an excess of boron trichloride in combination with tetra-*n*-butylammonium iodide (*n*-Bu$_4$NI) and shortened reaction times produced *N*-benzyl-2,7-di-*tert*-butyl-3,6-dihydroxycarbazole (**92**), selectively. All the reactions proceeded with high yields and the products were purified by either crystallization or trituration, with the exception of the demethylation step, where column chromatography was necessary.[6b,34]

The *N*-substituted 3,6-dihydroxycarbazoles **91** and **92** are important intermediates in the advancement of all of our subsequent work with azatrioxa[8]circulenes and diazadioxa[8]circulenes. They can be readily condensed with electron-rich 1,4-benzoquinones and 1,4-naphthoquinone to form asymmetrical and symmetrical azatrioxa[8]circu-

Scheme 19 Synthesis of *N*-substituted 2,7-di-*tert*-butyl-3,6-dihydroxy-carbazoles **91** (R = propyl) and **92** (R = benzyl). a: R = propyl. b: R = benzyl[6b]

Scheme 20 Synthesis of unsymmetrical azatrioxa[8]circulenes **93** and symmetrical azatrioxa[8]circulenes **94**.[34] **91**: R = propyl. **92**: R = benzyl
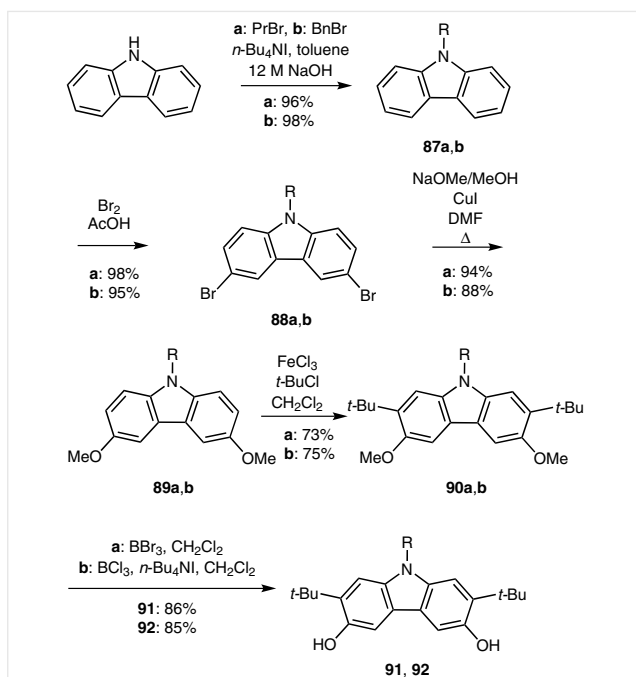
lenes **93** and **94** as presented in Scheme 20.[34] We have shown that the azatrioxa[8]circulene is formed in a stepwise fashion, where two intermediates could be isolated (Scheme 21). On treating 3,6-dihydroxycarbazole **92** with one equivalent of an electron-rich 1,4-benzoquinone (or 1,4-naphthoquinone), and boron trifluoride–diethyl ether complex, one carbon–carbon bond is formed. We presume that the coupling takes place via a Michael-type addition. If an electron-poor 1,4-benzoquinone (Cl, Br, CN) is used, oxidation of the dihydroxycarbazole is preferred over Michael
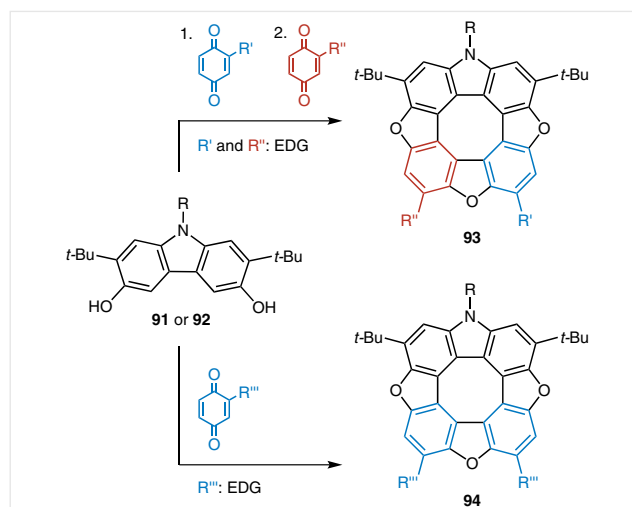
addition, which causes the dihydroxycarbazole to dimerize, forming diazadioxa[8]circulene **104**. This dimerization reaction is described in section 5. After further treatment with a Lewis acid and an oxidizing agent (chloranil), a furan ring (structure **96**) is formed from the condensation of two phenols, presumably via a quinoid intermediate. Addition of a second 1,4-quinone in the presence of boron trifluoride–diethyl ether complex yields an azatrioxa[8]circulene **93**. The second 1,4-quinone may be different to the one already attached, resulting in an unsymmetrical azatrioxa[8]circulene. This cyclic trimerization reaction of 3,6-dihydroxycarbazole **91** and two 1,4-quinones can be carried out in a stepwise manner with isolation of the intermediates, or in one-pot, to afford similar yields. In total, three new carbon–carbon bonds and three furan rings are formed, releasing three molecules of water.[6b,34]

Figure 8 Azatrioxa[8]circulenes synthesized by Pittelkow and co-workers in 2015
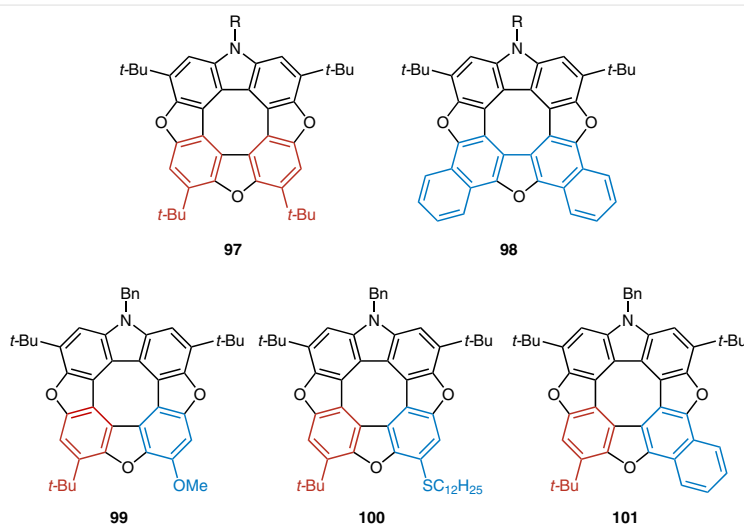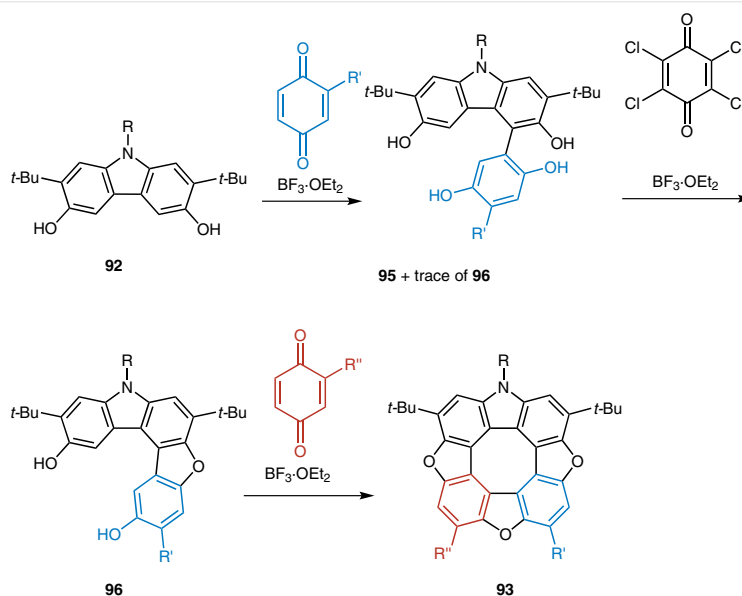
Scheme 21 Formation of unsymmetrical azatrioxa[8]circulene **93**. Tetrahydroxy compound **95** and dihydroxy compound **96** are intermediates

Under the stated conditions for the formation of circulenes, we found that when reacting dihydroxycarbazoles **91** or **92** with either 2-*tert*-butyl-1,4-benzoquinones or 2-methoxy-1,4-benzoquinones, only one regioisomer of the furan compound **96** was formed, as predicted by Erdtman's model (see Scheme 7, section 3).[20a] In this case the electron-donating group (EDG) (R′: blue) resides *ortho* to the hydroxy group as shown in Scheme 21. This led to the remarkable regioselectivity of the quinone substituents in the azatrioxa[8]circulenes **97**, **99**, **100** and **101**, which were produced in good yields with only traces of the regioisomers being present (Figure 8).[34] It also became apparent that the reaction of 3,6-dihydroxycarbazole **92** with 2-*tert*-butyl-1,4-benzoquinone and 2-methoxy-1,4-benzoquinone always gave one regioisomer of azatrioxa[8]circulene **99**, independent of the addition order. In the case of reacting **91** or **92** with 2-*tert*-butyl-1,4-benzoquinone and 1,4-naphthoquinone, the order of addition did influence the outcome of the reactions; when first reacting with the 2-*tert*-butyl-1,4-benzoquinone and later with 1,4-naphthoquinone, only one regioisomer, **102**, was isolated (Figure 9).[34] A reversed reaction order yielded a mixture of the two regioisomers as depicted in Figure 9.

The crystal structures shown in Figure 10 highlight the almost completely planar character of **97** and **98**, as predicted by our geometry model (see Figure 4, section 1). The 1,4-naphthoquinone-derived product **98** features significant π–π stacking between neighboring molecules and their naphthalene moieties. The molecules are stacked alternatingly with respect to the nitrogen atoms, to accommodate the *tert*-butyl and propyl groups, thereby creating
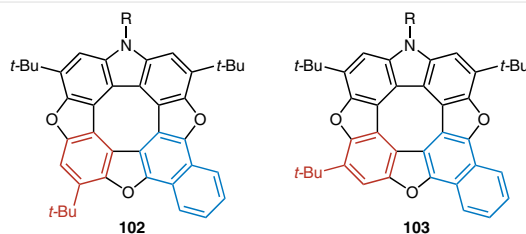
Figure 9 The two regioisomers obtained from the condensation of 3,6-dihydroxycarbazole **91** or **92** with 1,4-naphthoquinone and 2-*tert*-butyl-1,4-benzoquinone
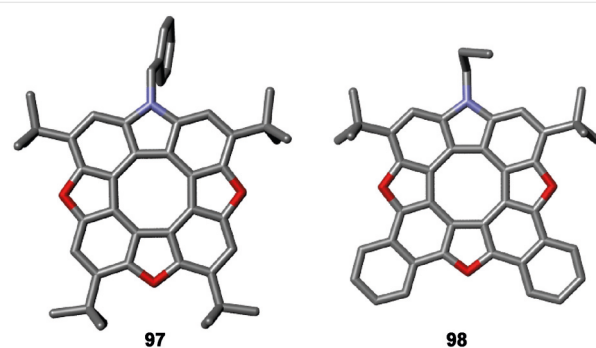
Figure 10 X-ray crystal structures of azatrioxa[8]circulenes **97** and **98**

diagonal stacks. On the other hand, azatrioxa[8]circulene **97** contains four *tert*-butyl groups which prevent π–π stacking. This results in an increased distance between the π-systems of neighboring molecules in the crystal structure.[6b,34]

5   Synthesis of Diazadioxa[8]circulenes

Similar to azatrioxa[8]circulenes, the synthetic logic behind the formation of diazadioxa[8]circulenes arises from the dihydroxydibenzofuran formed in the condensation of 1,4-quinone.[6c] In the synthesis at hand, 3,6-dihydroxycarbazole is oxidized with a fully substituted 1,4-benzoquinone to prevent any coupling reactions of the carbazole with the 1,4-benzoquinone. This results in dimerization of the 3,6-dihydroxycarbazole **86** which, assisted by a Lewis acid, leads to formation of a furan ring. Scheme 22 depicts the retrosynthesis of diazadioxa[8]circulenes **104**.
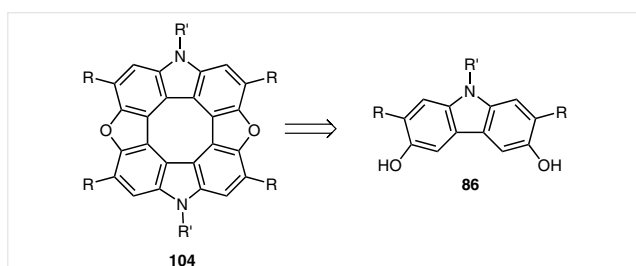
Scheme 22 Retrosynthesis of diazadioxa[8]circulenes **104**

The oxidative coupling of hydroxycarbazoles represents a type of aryl coupling reaction that is well known and widely used in organic chemistry.[35] The procedure usually requires an electron-rich aromatic system, often containing a hydroxy group, which is treated with an oxidizing agent.

In 2002, Botman studied the oxidative coupling of hydroxycarbazoles with a copper(II) sulfate (CuSO$_4$) catalyst on an alumina (Al$_2$O$_3$) support and dioxygen as the oxidant.[36] While other catalytic systems such as [Mn(acac)$_3$], [CuCl(OH)]·TMEDA, or VO(acac)$_2$ gave similar yields and selectivity, they required a more laborious product purification process. The reaction catalyzed by CuSO$_4$/Al$_2$O$_3$ was chosen for its facile purification. The pure symmetrically

bound carbazole dimer **108** was named BICOL (analogous to BINOL). It was proposed to function as a chiral bidentate ligand in homogenous asymmetric catalysis. The short synthetic pathway to this carbazole dimer is presented in Scheme 23.

Tetrahydrocarbazole[37] **105** was oxidized with wet deactivated palladium-on-carbon in the high boiling solvent *p*-cymene, giving mainly methoxycarbazole **106** and about 1% of 9*H*-carbazole. Demethylation with concentrated hydrobromic acid yielded hydroxycarbazole **107**. This compound was dimerized with copper(II) sulfate on an Al$_2$O$_3$ support with dioxygen as the oxidizing agent. Enantiomeric resolution of the dimer resulted in (+)- and (−)-BICOL. A drawback of the described oxidative aryl coupling method and similar methods is their unspecific nature, resulting in the formation of regioisomers. A recent study by Kozlowski and coworkers attended to the problem of regioselectivity in oxidative coupling reactions of monohydroxycarbazoles.[38] They presented known coupling reactions and a novel cata-
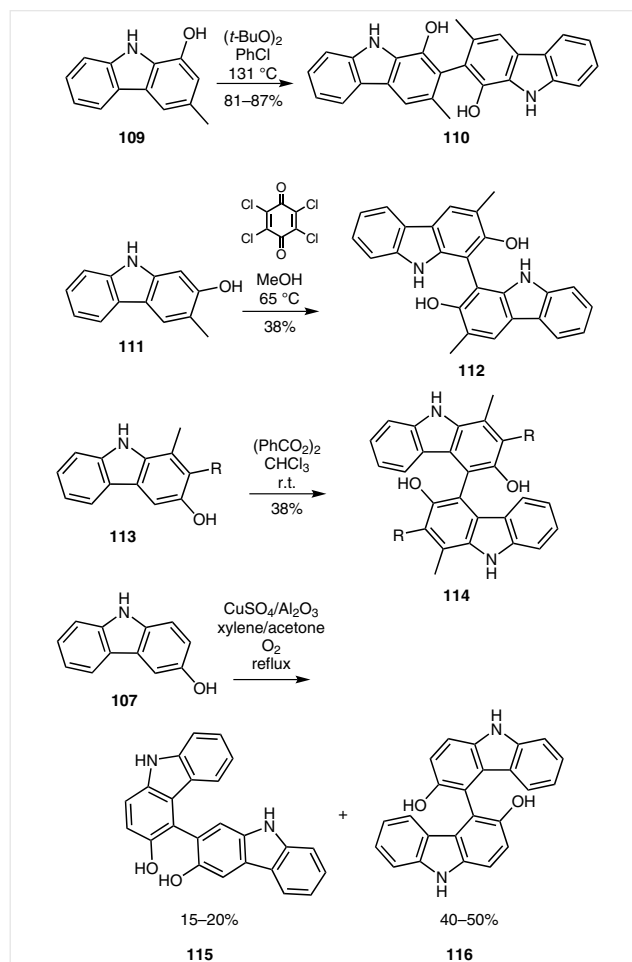
Scheme 24 Oxidative coupling reactions of hydroxycarbazoles exhibiting low regioselectivity[38]

Scheme 23 Synthesis of the hydroxycarbazole dimer, BICOL (**108**). Oxidative coupling also gave the 4–2′ bound product in 15–20% yield[36]

T. Hensel et al.

lytic system for regioselective couplings. The examples they gave on non-regioselective oxidative coupling reactions are presented in Scheme 24.

In a comparison between the different reagents and conditions in the oxidative coupling of *N*-methyl-2-hydroxycarbazole, only *tert*-butylperoxide gave moderate yields (1–3′ bond: 32%, 1–1′ bond: 29%); the use of manganese dioxide (MnO$_2$) resulted in lower yields (1–3′ bond: 20%, 1–1′ bond: 18%), with other conditions giving even worse yields. In an attempt to solve the low regioselectivity problem, many transition-metal salen and salan catalysts were screened. A vanadium catalyst, depicted in Scheme 25, was found to optimize both the yields and regioselectivity. Besides the main product **119**, small amounts of compound **118** (1–8%) and a major side product in the form of the tetramer **120** (9–30%) were observed.

They proposed a radical mechanism including reduction of vanadium from V(V) to V(IV), followed by regeneration of the catalyst by dioxygen. To validate their assumption, 2,2,6,6-tetramethylpiperidine 1-oxyl (TEMPO) was added to the reaction, inhibiting oxidative coupling. Exclusion of dioxygen also resulted in lower yields and inhibited formation of the tetramer.

In our recent work we showed that regioselectivity was not an issue, since the reactive 2- and 7-positions were blocked by *tert*-butyl groups. We reported a condensation reaction of two N-substituted 2,7-di-*tert*-butyl-3,6-dihy-

droxycarbazoles, **91** and **92**, mediated by an oxidizing agent (chloranil or 2,3-dichloro-5,6-dicyano-1,4-benzoquinone) and a Lewis acid (BF$_3$·OEt$_2$, AlCl$_3$ or FeCl$_3$) in dichloromethane (Scheme 26).[6c]
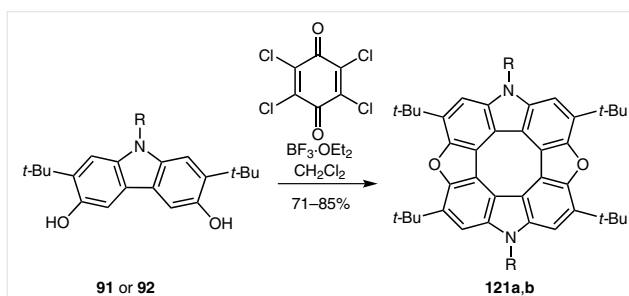
Scheme 26 Oxidative dimerization of *N*-substituted 2,7-di-*tert*-butyl-3,6-dihydoxycarbazole. Blocking the 2- and 7-positions resulted in high yields. **a**: R = propyl. **b**: R = benzyl
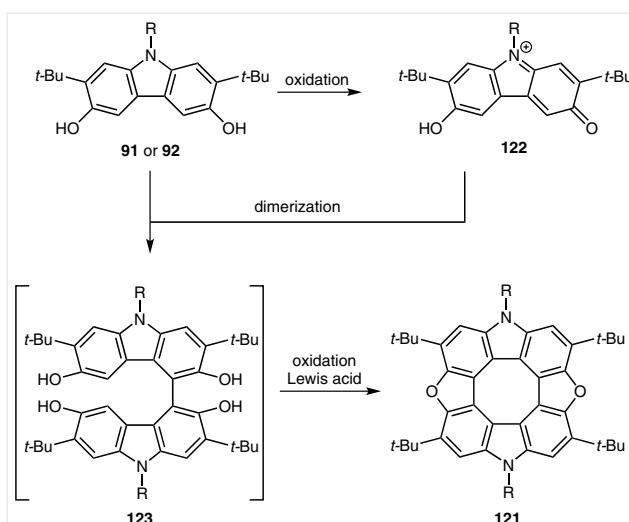
Scheme 27 Proposed reaction pathway for the oxidative condensation of 3,6-dihydroxycarbazole **91** or **92** to form diazadioxa[8]circulene **121**

Scheme 25 Regioselective oxidative coupling of substituted hydroxycarbazoles **117** with vanadium catalysis[38]
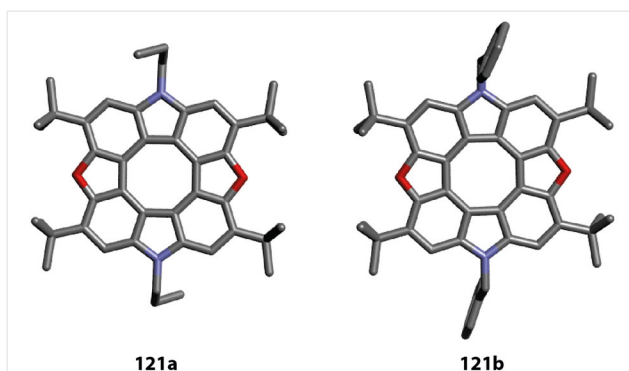
Figure 11 X-ray crystal structures of diazadioxa[8]circulenes **121a** and **121b**

We assumed that the oxidized form of the carbazole with a quinoid substructure **122**, as shown in Scheme 27, is an intermediate in this transformation. The 3,6-dihydroxy-carbazoles **91** or **92** dimerize with the oxidized compound **122** via a Michael-type addition, forming tetrahydroxycarbazole dimer **123**, which can be isolated. Addition of the Lewis acid, boron trifluoride–diethyl ether complex in the presence of chloranil led to the formation of diazadioxa[8]circulene **121**.[6c]

The mechanism of the initial oxidation step can proceed via a one- or two-electron transfer. Experimental data has shown that the presence of chloranil is necessary for the formation of the carbon–carbon bond. In a Michael-type addition process, the π-system of a hydroxy-substituted carbazole attacks the β-position of the quinoid oxidized carbazole **122**. After rearomatization and loss of two protons, the dimer **123** is formed. We assume that a second oxidation and carbon–carbon bond formation occurs, followed by two condensation reactions mediated by the boron trifluoride–diethyl ether complex to form the furan rings. In total, two carbon–carbon bonds and two oxygen bridges are formed and two molecules of water are eliminated, resulting in diazadioxa[8]circulene **121**.

To unequivocally prove that the main products of the dimerization of two molecules of 3,6-dihydroxycarbazoles **91** or **92** are the structures shown, single crystals of **121a** (R = propyl) and **121b** (R = benzyl) were grown by slow evaporation of dichloromethane from a mixture of dichloromethane–ethanol (1:1) (Figure 11). The resulting pale yellow needles were suitable for single-crystal X-ray crystallography.

Both diazadioxa[8]circulene derivatives **121a,b** are almost completely planar with small deviations in the bond lengths at the COT center of the molecule, being comparable to those in tetraoxa[8]circulenes (1.40–1.44 Å). Even though a large flat cyclic conjugated system is apparent, there is no π–π stacking visible due to the presence of the four *tert*-butyl substituents.[6c]

6   Synthesis of Other Heterocyclic [8]Circulenes

Besides tetraoxa-, azadioxa- and diazadioxa[8]circulenes, a number of systems that qualify as hetero[8]circulenes have been described in the literature. Only compounds with a planar COT core, fully cyclo-annulated by aromatic rings of which at least one is a heterocycle, qualify as hetero[8]circulenes.

One of the first sulfur-containing hetero[8]circulenes was described in 2006 by Nenajdenko and co-workers.[39] Their octathia[8]circulene **8** consists of eight thiophene moieties, *ortho*-fused to form the COT core. The name sul-

Scheme 28 Synthesis of sulflower (**8**) starting from 3,4-dibromothiophene[39]
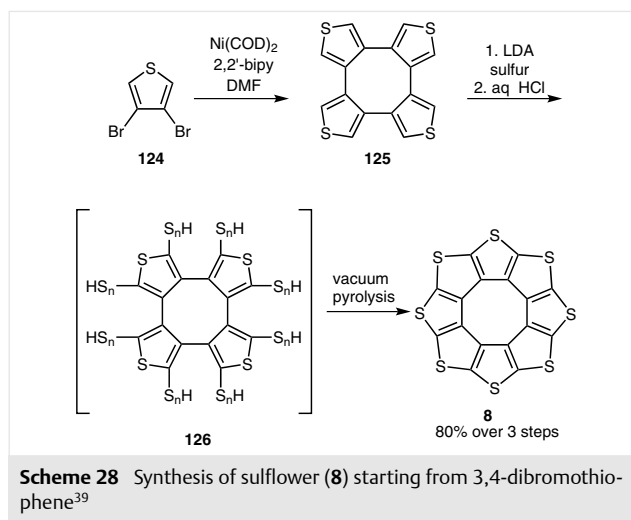
flower was chosen for its resemblance to the bloom of a sunflower. To prepare compound **8**, a short synthesis was employed as presented in Scheme 28.

The first step was a dehalogenative carbon–carbon coupling catalyzed by zerovalent nickel: 3,4-dibromothiophene (**124**) was reacted with bis(cyclooctadiene)nickel [Ni(cod)$_2$] having 2,2′-bipyridine as the ligand to form the cyclic tetramer **125**. Under strongly basic conditions, achieved with excess lithium diisopropylamide (LDA), cyclotetrathiophene **125** was treated with elemental sulfur. After acidic work-up, the tetrathiophene product **126** with all hydrogens replaced by polythiolates was formed. The octapolythiol-tetrathiophene **126** was converted into octathia[8]circulene **8** by vacuum pyrolysis. In a more recent paper, Nenajdenko described the synthesis of tetrathiatetraselena[8]circulene by simply replacing the sulfur powder in their previous synthesis with selenium powder.[6f] Elemental analysis, high-resolution mass spectrometry and NMR spectroscopy confirmed the identity and structure of octathia[8]circulene **8**. Final structural proof was obtained in the form of matching calculated and experimental single-crystal X-ray data. Sulflower is a highly symmetrical and planar molecule with dense crystal packing. Nenajdenko emphasized the importance of the electronic properties of organosulfur compounds,[39] since they are possible candidates for organic light-emitting devices,[40] thin-film transistors[41] and other applications.[42]

In the same year, Osuka and co-workers described a tetrameric porphyrin sheet with an embedded tetraaza[8]circulene subunit.[6g] This porphyrin sheet was prepared, starting with a Rothemund synthesis, where pyrrole condensates with two molecules of an aldehyde and a pyrrole trimer under acidic conditions. Addition of 2,3-dichloro-5,6-dicyano-1,4-benzoquinone (DDQ) resulted in oxidation and reconjugation of the π-system. Multiple reaction steps consisting of coupling reactions with silver hexafluoro-
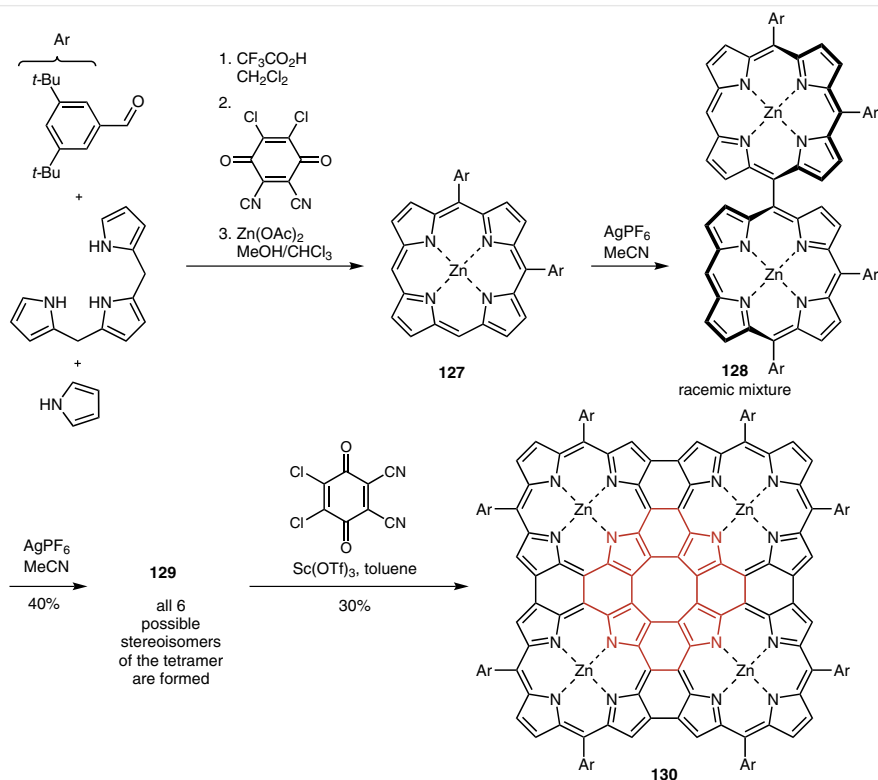
Scheme 29 Synthesis of porphyrin tetramer **130**. The tetraaza[8]circulene subunit with a COT core is highlighted in red[43]

phosphate (AgPF$_6$) in acetonitrile and enantiomeric resolutions, followed by oxidation with a mixture of DDQ and scandium(III) triflate [Sc(OTf)$_3$] in toluene, gave the porphyrin sheet **130** in low yield. A more efficient synthesis (Scheme 29), was introduced by Osuka and co-workers two years later.[43] In their more recent work, they refrained from using enantiomeric resolution after the dimerization and tetramerization steps (with AgPF$_6$ in MeCN).

The aromaticity of the porphyrin subunits and the antiaromaticity of its central COT were studied extensively by NMR spectroscopy, theoretical methods [nucleus-independent chemical shift calculations (NICS)], optical spectroscopy and electrochemical methods. Geometry optimizations, performed by Osuka, depict a completely planar porphyrin sheet and central COT.[6g] The COT core was shown to have a strongly antiaromatic character, while the zinc–porphyrin subunits retained a weakened aromatic character. Ligand binding studies aimed at examining aromaticity and antiaromaticity are presented in section 8 of this account.

Recently, Wong and co-workers introduced a short synthetic route to form tetrathia- **133** and tetraseleno[8]circulene **134** starting from octamethoxytetraphenylene **131**.[44] Starting material **131** was prepared via two-step syntheses starting from either 2,2′-dibromo-4,4′,5,5′-tetramethoxybiphenyl or 2,2′-diiodo-4,4′,5,5′-tetramethoxybiphenyl.[45] The synthesis of the cyclic sulfur- and selenium-bridged tetraphenylenes is presented in Scheme 30.
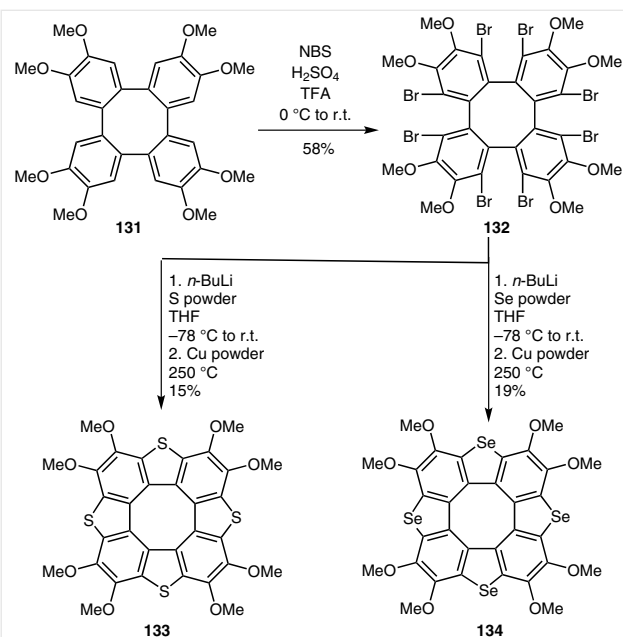
Scheme 30 Synthesis of tetrathia[8]circulene **133** and tetraseleno[8]circulene **134** derived from cyclic octamethoxytetraphenylene **131**[44]

Tetraphenylene **131** was reacted with *N*-bromosuccinimide (NBS) in trifluoroacetic acid (TFA) and sulfuric acid (H$_2$SO$_4$) to achieve an eight-fold bromination. The resulting

octabromide **132** was lithiated with an excess of *n*-butyl-lithium (*n*-BuLi), replacing all the bromine atoms. The subsequent addition of selenium or sulfur powder led to the polyselenolate or polythiolate intermediate, respectively. Finally, thermal treatment (250 °C, under argon) of the intermediates with copper powder yielded the hetero[8]circulenes **133** and **134**. Single crystal X-ray data revealed tetraphenylene **131** and tetraselena[8]circulene **134** were saddle-shaped, while tetrathia[8]circulene **133** was completely planar. This disparity arose due to the difference in bond lengths of the C–Se bonds (1.86 Å) and the C–S bonds (1.72 Å) in the respective tetrahetero[8]circulenes. The crystal structures also showed no π–π stacking interactions, as these were prevented by the methoxy groups. Weak C–H···π interactions were however observed (~2.8–3 Å). Analysis of the optical properties by UV/Vis and fluorescence spectroscopy revealed a λ_{max} red shift of the circulenes compared to tetraphenylene **131**. A λ_{max} red shift of the seleno compound **134** compared to the sulfur compound **133** was also observed, with both circulenes displaying similarly shaped spectra. In accordance with UV/Vis spectroscopy, their cyclic voltammograms displayed relatively small highest occupied molecular orbital–lowest unoccupied molecular orbital (HOMO–LUMO) gaps. The investigations on the aromaticity and antiaromaticity, including the calculated NICS values, are presented in section 8 of this account.

Very recently, Osuka and co-workers reported on the synthesis of a tetraaza[8]circulene, the first of its kind.[46] The synthetic protocol employed an oxidative fold-in fusion reaction, where a 1,2-phenylene-bridged cyclic tetrapyrrole was converted into tetranaphthotetraaza[8]circulene in 96% yield. X-ray diffraction data confirmed the planarity of the product, which is important in the study of antiaromaticity.

7   Synthesis of Structurally Related Compounds

The compounds described in this section feature, in contrast to the hetero[8]circulenes, a partly annulated COT core. They are either derivatives of the cyclic versions of tetraphenylene, tetrathiophene or dithienophene.

An early example was described by Hellwinkel and Reiff in 1970.[61] They produced a compound with a presumably planar COT core, annulated by four benzene rings which were themselves connected by methylene bridges. The synthetic pathways resulting in tetramethano-*o*-tetraphenylene **14** and trimethano-*o*-tetraphenylene **143** are depicted in Scheme 31.

Scheme 31 Synthesis of tetramethano[8]circulene **14** and trimethano-*o*-tetraphenylene **143**[61]
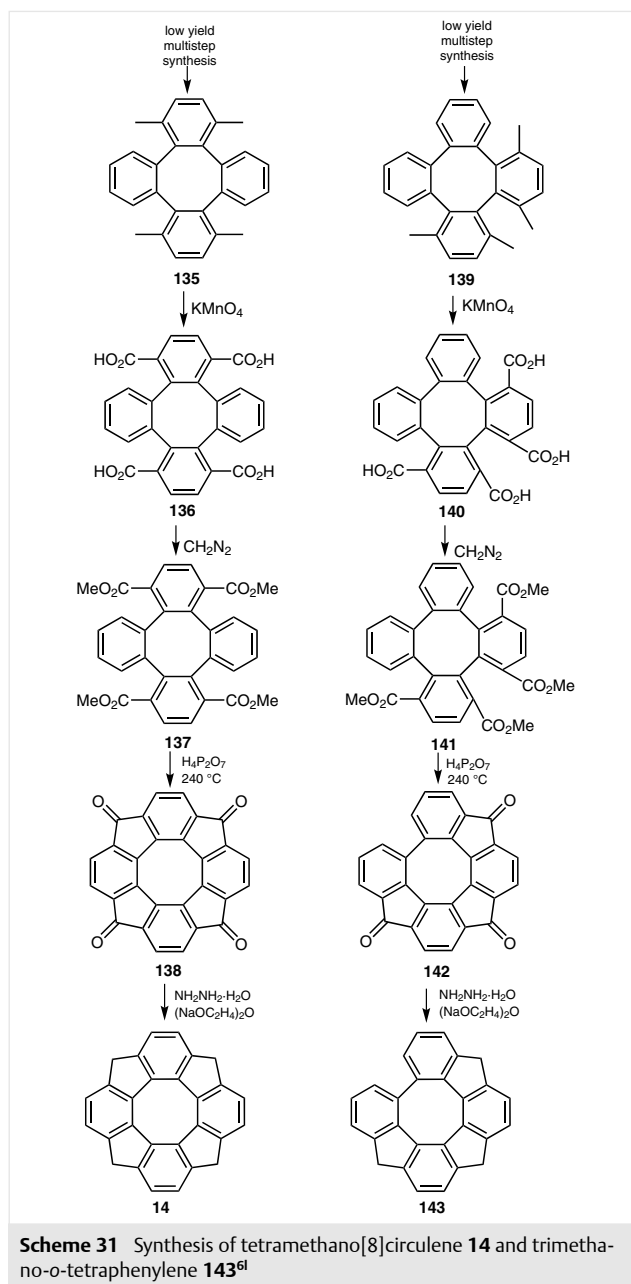
The starting materials, tetramethyltetraphenylenes **135** and **139**, accessible by a low-yielding multistep synthesis, were first oxidized with potassium permanganate (KMnO₄) to yield the tetracarboxylic compounds **136** and **140**.[47] Treatment with diazomethane produced the corresponding methyl esters **137** and **141**, which were reacted with polyphosphoric acid. The obtained cyclic fluorenones **138** and **142** yielded tetramethano-*o*-tetraphenylene **14** and tri-

methano-o-tetraphenylene **143** when reduced with hydrazine in sodium diethylene glycolate. The products were assumed to be planar based on steric considerations.

In 2010, attempting to create cyclo-annulated planar COT systems, Iyoda and co-workers[45] published the synthetic routes for three different cyclic tetrathiopenes with either two dimethylsilyl, two sulfur or two sulfoxide bridges on opposite sides of the compounds, respectively. The reaction pathways are shown in Scheme 32.
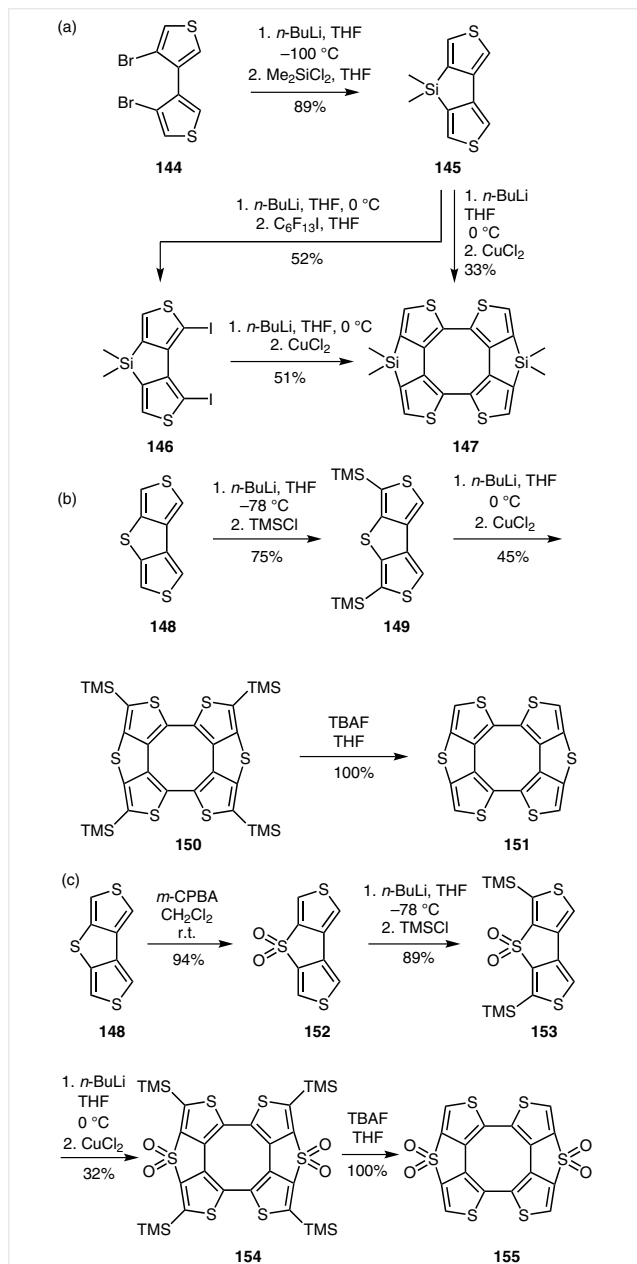
Scheme 32 Synthesis of bridged tetrathiophenes. (a) Silyl-bridged **147**. (b) Sulfur-bridged **151**. (c) Sulfoxide-bridged **155**[45]

Silyl-containing cyclic tetrathiophene **147** was synthesized, starting with a dilithiation of dibromo-dithiophene **144** and subsequent treatment with dichlorodimethylsilane to give **145**. Dimerization to form **147** was achieved by dilithiation, reaction with tridecafluorohexyl iodide and reacting the obtained diiodide **146** with n-BuLi and copper(II) chloride (CuCl$_2$). Directly reacting **145** with n-BuLi and CuCl$_2$ yielded product **147** as well. The sulfur-bridged cyclic tetrathiophene **151** and the sulfoxide-bridged cyclic tetrathiophene **155** both originated from dithienothiophene **147**, which was described in an earlier paper by Yoshida, Iyoda and co-workers.[48] Bis(4-bromothiophen-3-yl)sulfane was converted into dithienothiophene **148** via a palladium-catalyzed cyclization. To produce the sulfur-bridged COT compound **151**, dithienothiophene **148** was selectively dilithiated and reacted with trimethylsilyl chloride (TMSCl) to give compound **149**, which was itself dilithiated again and treated with CuCl$_2$ to yield the trimethylsilyl-protected cyclic dimer **150**. Deprotection with tetrabutylammonium fluoride (TBAF) resulted in the cyclic tetrathiophene **151** with two opposing sulfur bridges. The same reaction pathway was applied to give the oxidized cyclic tetrathiophene **155**. Oxidation with m-chloroperoxybenzoic acid (MCPBA) was required, preceding the TMS protection step. The single crystal X-ray and calculated optimized structures concurred concerning the planarity of the molecules. The sulfur-bridged compound **151** was the most planar (bent angle: 4.3°), followed by the sulfoxide-bridged compound **155** (7.0°) and the dimethylsilane-bridged compound **147** (19°).

Following these findings, the magnetic ring currents and HOMO–LUMO energy gaps have been studied by NMR spectroscopy, UV/Vis spectroscopy and cyclic voltammetry (CV). In the proton NMR spectrum, the α-protons of all the heteroatom-bridged cyclic tetrathiophenes (**147**: δ 7.26, **151**: δ 6.97 and **160**: δ 7.99) experienced an upfield shift compared to the corresponding dimeric analogs (**145**: δ 7.53, **148**: δ 7.39 and **152**: δ 8.29). However, the α-protons of saddle-shaped cyclic tetrathiophene without bridging heteroatoms (δ 7.37) experienced a downfield shift compared to 3,3′-bithiophene (δ 7.20). A distinct trend became apparent: the compounds with the highest planarity experience the highest upfield shifts. The shifts presumably originate from a paratropic ring current induced by the COT core. Decreased diatropicity of the thiophene rings as the cause was ruled out by comparison of the NICS values and the differences in chemical shift values of the synthesized compounds and a few related compounds. Comparing the colors of solutions of the tetrathiophenes gave an indication of the differences in the HOMO–LUMO gap size: the silyl compound **147** was orange (λ$_{max}$ = 483 nm) in solution, the oxidized sulfur compound **155** was red (λ$_{max}$ = 575 nm), and the sulfur compound **151** was purple (λ$_{max}$ = 618 nm). The increasing planarity of the molecules was accompanied by a decreasing HOMO–LUMO gap size, which was in accordance with the CV results.

T. Hensel et al.

Iyoda's idea of thiophene-annulated cyclooctatetraenes was further pursued by Nishinaga et al., who in 2013 published their work on the synthesis of dithienophene compounds with a planarized COT core and with directly attached protons.[49] The synthetic pathway toward dithieno-thiophene-COT **161** comprised six steps (Scheme 33).
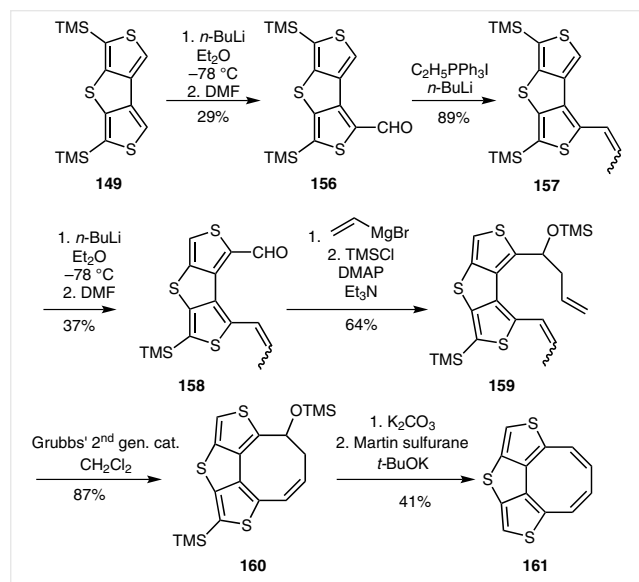
Scheme 33 Synthesis of dithienophene-annulated cyclooctatetraene **161**[49]

In the first reaction, dithieno[3,4-*b*:3′,4′-*d*]thiophene **149** was formylated by lithiation with *n*-BuLi in diethyl ether (Et$_2$O) followed by addition of *N,N*-dimethylformamide (DMF). The resulting aldehyde **156** underwent a Wittig reaction to form propylene **157**. After a second formylation, and a subsequent Grignard reaction with vinylmagnesium bromide, diene **159** was formed. The alkene moieties in **159** were utilized in a metathesis reaction with the second generation Grubbs catalyst to yield the cyclooctatriene **160**. Finally, elimination of TMS under oxidative conditions (Martin sulfurane) with potassium *tert*-butoxide (*t*-BuOK) yielded the dithienothiophene-COT **161**. X-ray and NMR data, as well as the calculated structure and NICS values indicated a planar compound **161** with a magnetically antiaromatic COT-core. The protons attached directly to the COT core experienced a paratropic ring current and the magnetic antiaromaticity was higher than in the previous tetrathiophenes presented by Iyoda in 2010.[45] Optical spectroscopy and cyclic voltammetry revealed a considerably smaller HOMO–LUMO gap. The analytical data concerning the magnetic antiaromaticity of the COT is further discussed in section 8 of this account.

In 2014, Wong and co-workers described the synthetic pathways for the preparation of diheteroatom-bridged tetraphenylenes with oxygen, nitrogen, sulfur and selenium bridges.[50] Their synthesis of dioxatetraphenylene **169** re-

quired cyclic tetraphenylene **168** as the starting material, which was obtained by a procedure described in their previous work from 2005 (Scheme 34).[6h]

Tetratriflate **168** was reported to be the main product in a synthetic pathway starting with an Ullmann coupling of two molecules of 2-iodo-3-nitroanisole (**162**) with copper bronze in nitrobenzene at 190–200 °C. 2,2′-Diamino-6,6′-dimethoxybiphenyl (**164**) was then obtained by reducing the nitro groups of biphenyl **163** with zinc and hydrochloric acid.[51] The conversion of the amines into iodides was accomplished by treatment with sodium nitrite in hydrochloric acid followed by addition of potassium iodide (KI) to give **165**. After dilithiation of **165** and addition of *N,N,N′,N′*-tetramethylethylenediamine (TMEDA), the dilithium intermediate was oxidatively coupled in the presence of CuCl$_2$ to form cyclic tetramethoxytetraphenylene **166**. Deprotection of the methyl groups with boron tribromide followed by treatment with triflic anhydride (Tf$_2$O) and pyridine yielded tetratriflate **168**.

As shown in Scheme 35, tetratriflate **168** was found to undergo an intramolecular reaction forming two furan rings upon treatment with tetrakis(triphenylphosphine)palladium(0) [Pd(PPh$_3$)$_4$] and potassium phosphate (K$_3$PO$_4$) in DMF at 140 °C for 24 hours. Wong et al. assumed that trace amounts of water partially hydrolyzed the triflate

Scheme 34 Synthesis of tetratriflate **168**, a precursor of dioxatetraphenylene **169**[6h,51]

T. Hensel et al.

in the starting material. The resulting hydroxy group caused intramolecular coupling to form the furan moieties in **169**. The synthesis of the nitrogen-, sulfur-, and selenium-bridged compounds **171**, **173**, **174** and **176** (Scheme 35) required a different starting material, 1,8,9,16-tetrabromotetraphenylene (**170**). It was prepared in two steps from 2,2′,6,6′-tetrabromobiphenyl, as described by Iyoda and Kabir.[52] At first, tetrabromobiphenyl was lithiated, followed by reaction with zinc(II) bromide to form dibenzozincacyclopentadiene. In a second reaction, 1,8,9,16-tetrabromotetraphenylene (**170**) was obtained via dimerization involving catalysis with CuCl$_2$. Wong[50] utilized **170** in a reaction with sodium azide, copper(I) iodide (CuI) and *N,N′*-dimethylethylenediamine (DMEDA) at 120 °C in dimethyl sulfoxide (DMSO) to form di-9*H*-carbazole **172**, followed by reaction with benzyl bromide and sodium hydride in tetrahydrofuran to yield *N*-benzylated compound **173**. They also found that treatment of **170** with aniline, tris(dibenzylideneace-

tone)dipalladium(0) [Pd$_2$(dba)$_3$], sodium *tert*-butoxide (*t*-BuONa) and tri-*tert*-butylphosphine [(*t*-Bu)$_3$P] in toluene gave the *N*-phenyl-bridged tetraphenylene **171**. The sulfur- and selenium-bridged compounds were also derived from the tetrabromo compound **170**. Treatment of **170** with *n*-BuLi and iodine (I$_2$) in tetrahydrofuran, followed by CuI/DMEDA and potassium sulfide (K$_2$S) in acetonitrile (140 °C) resulted in the formation of two thiophene moieties in product **174**. When tetrabromide **170** was lithiated with *n*-BuLi and reacted with selenium powder in tetrahydrofuran (–78 °C), the obtained bis(diselenium)-bridged **175** product was subjected to thermal deselenation with copper powder (250 °C) to yield diseleno-bridged tetraphenylene **176**. Single-crystal X-ray structures and calculated structures indicated that all the diheteroatom-bridged tetraphenylenes were saddle-shaped, however, the bent angles were significantly smaller than those in tetraphenylene and decreased in the order Se > S > N > O. An exception was *N*-phenyltetraphenylene **171**, which had a significantly smaller bent angle (8.89°) than the other compounds (25.56° to 37.43°). It appeared that the cyclic tetraphenylene required more than two heteroatom bridges to achieve a fully planar structure. UV/Vis spectra revealed a red shift of the λ$_{max}$ for the heteroatom-bridged compounds compared to cyclic tetraphenylene. The shift of λ$_{max}$ appeared to be in an inverse relationship with the bent angles, in accordance with the results obtained by Iyoda.[45,50]

Tetramesitylene compound **182**, an all-carbon [8]circulene, was recently described by Tobe and Nakano.[53] The potential tetra-radicaloid system of **182** was investigated for its structure and electronic properties by the means of DFT calculations and experimental data. The synthetic pathway toward [8]circulene **182** is presented in Scheme 36.

Scheme 35 Synthesis of oxygen-, nitrogen-, sulfur-, and selenium-bridged tetraphenylenes[50]

Scheme 36 Synthesis of tetracyclopenta[*def,jkl,pqr,vwx*]tetraphenylene derivative **182**[53]
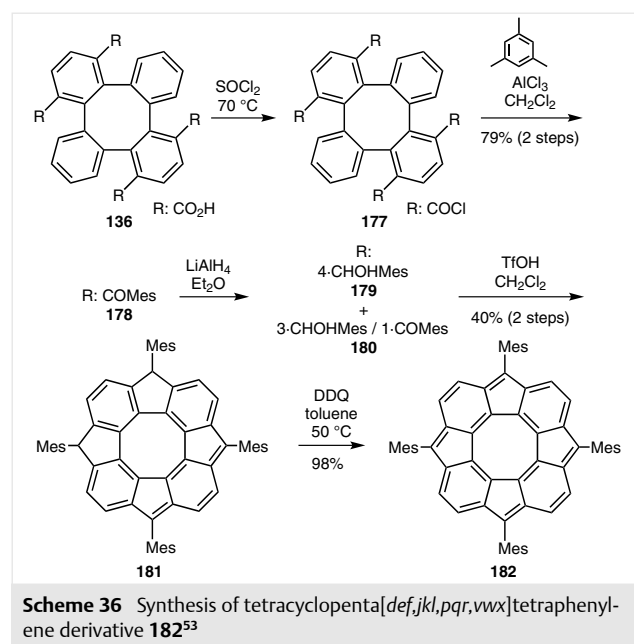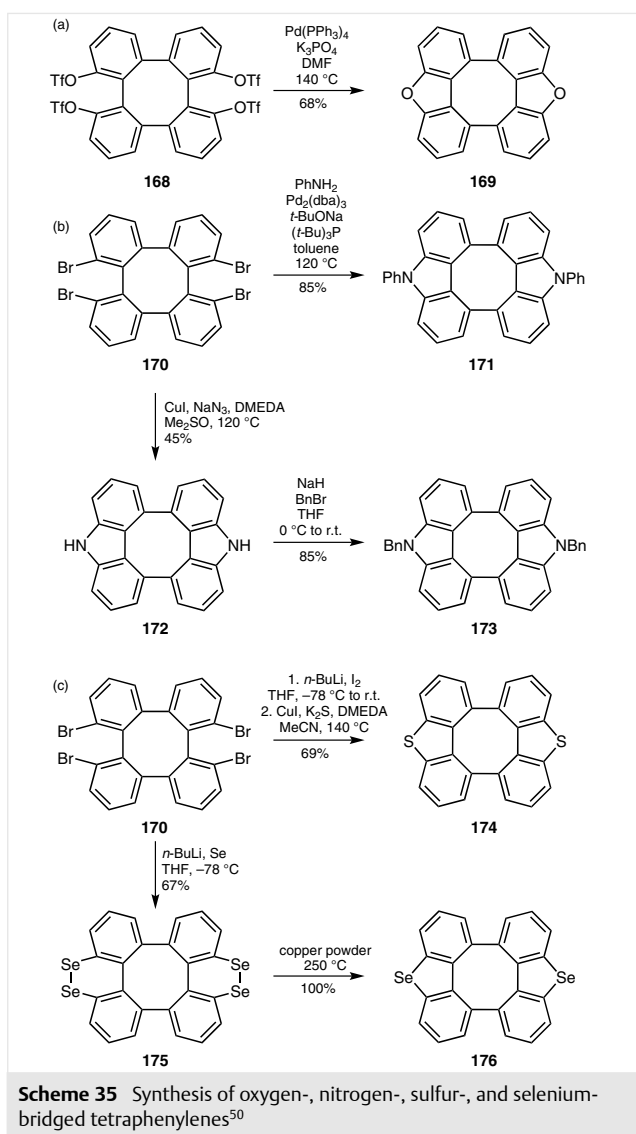
The starting material, tetracarboxylic acid **136**, was obtained via the literature procedure described by Hellwinkel and Reiff.[47b] After formation of the acid chloride **177** with thionyl chloride (SOCl$_2$), a Friedel–Crafts reaction with mesitylene and aluminum chloride yielded tetraketone **178**. Treatment with lithium aluminum hydride (LAH) resulted in a mixture consisting of the incomplete reduction product **180** and tetrahydroxy compound **179**. Addition of triflic acid gave the dihydro product **181**, which was subjected to oxidation with DDQ to yield 1,4,7,10-tetramesityltetracyclopenta[*def,jkl,pqr,vwx*]tetraphenylene **182**. Analysis of compound **182** by ^{1}H NMR spectroscopy revealed the proton signal of the tetracyclopentantetraphenylene ring to be significantly shifted upfield, at 2.85 ppm, indicating a strong paramagnetic shielding effect due to the central COT system and a considerably lowered aromaticity of the cyclo-annulated ring system. Tobe and Nakano's NICS(1) calculations supported these observations with a large positive value for the COT core (10.15), positive values for the quinone-like substructure (4.60) and cyclopentane ring (7.86), and a small negative value for the benzene-structured ring (–1.22). The single-crystal X-ray structure of compound **182** revealed a completely planar COT and an approximate D_{2h} structure. The COT core itself experiences significant bond length fluctuations.[53]

8 Hetero[8]circulenes and Related Compounds as Tools to Study Aromaticity and Antiaromaticity

The term aromaticity is most commonly used to describe a cyclic delocalized electron system. Defining aromaticity has been a daunting task, despite the numerous examples of compounds and the general perception that aromaticity equals stability. As such, its reciprocal concept, antiaromaticity, has proven even more difficult to study, as compounds designed with cyclic 4n π-systems often prefer bent structures and localized double bonds, as opposed to the planar, delocalized structures ideally needed for study. Arriving at a definition can be attempted by analyzing the four properties usually associated with aromaticity: reactivity, structural features, energetic properties and magnetic behavior, and compare these to how antiaromatic systems are expected to act. This section will mainly address the structural, energetic, and magnetic aspects.

Both aromatic and antiaromatic systems feature planar structures. The delocalization of electrons in aromatic compounds stabilizes the system energetically and chemically. For antiaromatic compounds, the delocalized double bonds, however, do not represent a minimum in energy, and as such, systems designed to be antiaromatic exhibit localized double bonds. Aromatic molecules feature a relatively large gap between the HOMO and LUMO,[54] which increases further with successive addition of aromatic rings.[55] The opposite is true for antiaromatic compounds: the localization of double bonds, and therefore absence of resonance stabilization leads to a smaller HOMO–LUMO gap. A consequence of the change in HOMO–LUMO gap size, and therefore electronic properties, is a change in optical properties, influencing the absorption and emission spectra. The altered electronic properties are of interest in the field of organic semiconductors, which require compounds with a small gap size.[56]

Classifying aromatic and antiaromatic systems by their magnetic behavior is possibly the most valuable property in discerning the concepts.[56] An overall diatropic ring current is characteristic for aromatic systems, and an overall paratropic ring current is representative for antiaromatic systems. Because of these inherent magnetic properties, NMR spectroscopy is a powerful tool to evaluate the aromatic or antiaromatic character of a molecule. The chemical shifts observed in proton NMR spectra can be associated with aromaticity in the case of a downfield shift caused by a diatropic ring current on the outside of the ring, or an upfield shift for nuclei positioned on the inside or above the ring. Due to the paratropic ring current of antiaromatic systems, these predictions are inversed. The magnetic properties of the ring current can also be predicted reasonably well by calculation of NICS values.[56] In this computational method, a ghost atom is placed in the center of a ring system (NICS(0)) or typically one Ångstrom above it (NICS(1)) to calculate the locally increased or decreased magnetic effect the ring system has on the ghost atom. Large negative values hint at local aromaticity, whereas large positive values indicate local antiaromaticity. Values around zero are likely to predict local non-aromatic properties. Similar sized ring systems can be compared directly, while systems of different sizes must take the ring size effect into account. It is also important to only compare NICS values that have been calculated at the same theoretical level. The curious properties and variations of aromatic and antiaromatic systems underline the importance of any investigation.[57]

One of the first tetra-annulated bicyclo COT systems was described by Richter et al. in 1991.[58] They explored the possibility of forming a planar dianionic COT despite steric hindrance. The synthesis of tetrakis(bicyclo[2.2.2]octane)cyclooctatetraene **184** is presented in Scheme 37, omitting the preparation of the dibromo tetramer **183**.[59]

Scheme 37 Synthesis of tetrakis(bicyclo[2.2.2]octane)cyclooctatetraene **184** and tris(bicyclo[2.2.2]octane)benzene **185**[58]
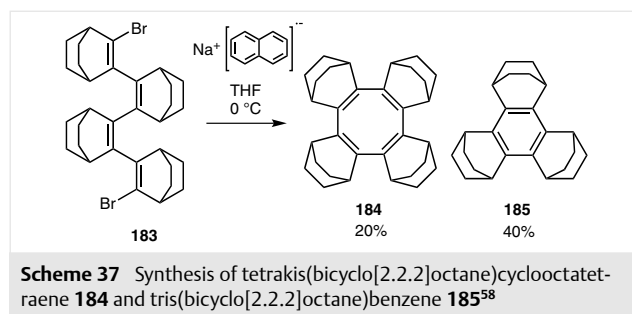
Dibromobicyclo[2.2.2]tetramer **183** was reacted with sodium naphthalenide in tetrahydrofuran at 0 °C yielding tetrabicyclo[2.2.2]-COT **184** (20%) and a larger amount of tribicyclo[2.2.2]benzene **185** (40%). Analysis of the single-crystal X-ray structure revealed bicyclo[2.2.2]octane **184** to be saddle-shaped, while benzene compound **185** featured a planar center. The ^{13}C NMR spectrum of bicyclo-annulated COT **184** showed four signals reflecting its D_{2d} symmetry. Optical spectroscopy revealed the typical UV/Vis absorptions of a COT chromophore. An interesting feature is represented by the possibility to produce the dianion by reduction with potassium mirror in tetrahydrofuran. The proton and carbon NMR spectra of the dianion of **184** imply planarity: the COT carbons are shifted upfield, the bridging ethylene carbons give one signal instead of two and the diatropic ring current causes a downfield shift of the bridgehead protons.

A decade later, another study concerning tetrabicycloalkane-annulated cyclooctatetraene and the corresponding benzene emerged. Tetrakis(bicyclo[2.1.1]hexane)cyclooctatetraene **193** and tris(bicyclo[2.1.1]hexeno)benzene **192** were synthesized in 2001 by Komatsu and co-workers (Scheme 38).[60] It was one of the first planar COT systems without an annulated aromatic system forcing it to planarity.
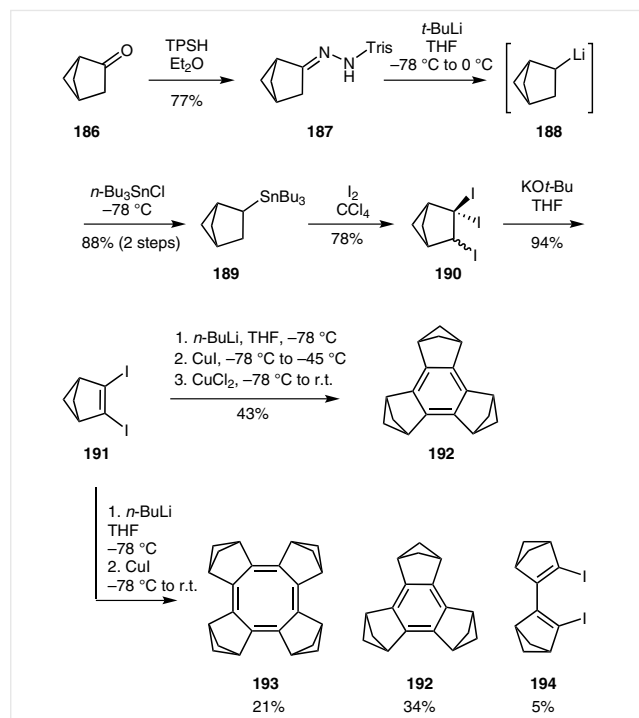
Scheme 38 Synthesis of tetrakis(bicyclo[2.1.1]hexane)cyclooctatetraene **193** and tris(bicyclo[2.1.1]hexeno)benzene **192**[60]

The synthetic route to cyclo-annulated COT **193** began with the reaction of ketone **186** with 2,4,6-triisopropylbenzenesulfonyl hydrazide (TPSH). The resulting product **187**

was then lithiated and reacted with tributyltin chloride (*n*-Bu$_3$SnCl) to yield bicyclo tributyltin derivative **189**. Treatment with iodine followed by oxidation with potassium *tert*-butoxide gave diiodide **191**. At this point in the synthetic pathway, the final reaction step could be optimized to either yield only tribicyclo benzene **192** (by lithiation, addition of CuI and CuCl$_2$) or to afford a mixture of tetrakisbicyclo COT **193**, trisbicyclo benzene **192** and a bicyclo[2.1.1] dimer **194** (by lithiation and addition of only CuI). When comparing the analytical data of the planar bicyclo[2.1.1]-COT **193** and the saddle-shaped bicyclo[2.2.2]-COT **184**, large differences became apparent. The UV/Vis spectra revealed a significant red shift of λ_{max} ($\Delta\lambda$ 177 nm = 7 eV) from saddle-shaped compound **184** (282 nm) to planar compound **193** (459 nm). The potential of both oxidation waves in the cyclic voltammetric studies increased by approximately 0.4 V from bicyclo[2.2.2]octane **184** to bicyclo[2.1.1]hexane **193**. Komatsu also compared the ^{1}H NMR spectra of the COT-core compound **193** with that of benzene-core compound **192**. The bridgehead hydrogen atoms were deemed to be influenced the most by the ring current from the COT core, since they are positioned in the same plane as the COT core. The observed difference in chemical shift however, was only 0.18 ppm. Calculated NICS values and magnetic susceptibility exaltations (Λ) indicated an aromatic benzene core in **192** (NICS value of –8.0 compared to –9.7 for D_{6h} benzene) and an antiaromatic COT in **193** (NICS value of 10.2 compared to 27.2 for standard planar D_{4h} COT), therefore a greater downfield shift, due to the paratropic ring current of the antiaromatic COT core, was expected.[60]

To study the antiaromaticity of an annulated planar COT system, Osuka and co-workers developed a synthetic pathway to form the porphyrin tetramer **130**.[6g] This porphyrin sheet incorporated a tetraaza[8]circulene moiety. In a series of papers ranging from 2006 to 2008, the magnetic ring-current effect of the COT core and the porphyrin subunits was analyzed by coordinating imidazoles and pyridines to the zinc atoms bound within the porphyrins.[40,61] The synthesis of a tetra-annulated porphyrin containing COT **130** is shown in Scheme 29 (see section 6). Both ligands (1,4-bis[(1-methyl-1*H*-imidazol-2-yl)ethynyl]benzene **195** and bis-methylimidazole porphyrin **196**) were shown to form 2:1 complexes with the porphyrin sheet. The imidazoles coordinated to two zinc atoms in the porphyrin sheet, causing them to be diagonally locked onto the COT core (Scheme 39). The resulting complexes were studied by ^{1}H NMR spectroscopy (the observed protons are marked in red in Scheme 39) and the results were compared to DFT calculations. When comparing the chemical shifts of the protons residing directly above the COT core from the bound and unbound ligands, large downfield shifts of 3.78 ppm for the linear ligand and 5.29 ppm for the porphyrin ligand became apparent. Osuka interpreted this observation as an effect of a strong paratropic ring current

Scheme 39 Complexation of Osuka's porphyrin sheet **130** with different ligands. Examined protons are highlighted in red. The differences in the proton chemical shifts between bound and unbound ligands for compounds **197–200** are presented next to the corresponding protons in ppm.[6g,61] The ligands below the porphyrin sheets are omitted for clarity
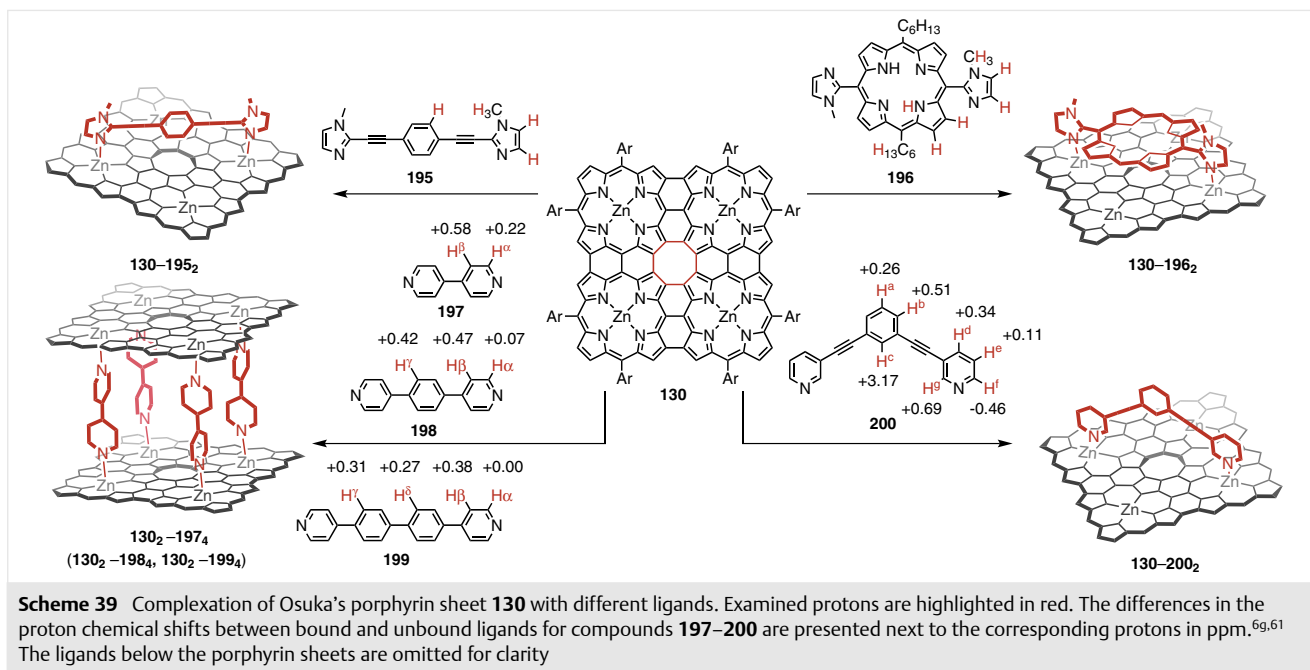
experienced by the aromatic protons in the complexed form, which led to strong magnetic deshielding. Protons located on top of the porphyrin moieties exhibited upfield shifts (–0.01 to –0.83 ppm), which were attributed to a weakened diatropic ring current above the zinc porphyrins. DFT calculations were conducted to gain understanding of the unusual chemical shift changes observed in the proton NMR spectra of the bound ligands. The NICS values, calculated for the COT core of the zinc(II) porphyrin tetramer (61.7) and the tetramer without zinc(II) (21.7), were large and positive, hinting at a strong paratropic ring current. The COT core was therefore assumed to have a magnetically strong antiaromatic character. Small positive and negative NICS values were calculated at the centers of different rings in the porphyrin subunits, suggesting substantially weakened aromaticity, down to a level where some of the rings could not be considered as being aromatic anymore. These small values (–1.1 to 2.8) stand in contrast to the large negative NICS values (–16.5 to –21.7) calculated for the individual porphyrin and magnesium porphyrin, which would indicate a strong aromatic character of the electronic system of the isolated subunits.[6g] It is assumed that the strong paratropic ring current of the COT core influences the 18π aromatic porphyrin systems, weakening them to the observed extend.

Subsequently, Osuka and co-workers presented additional investigations on the porphyrin sheet **130** with different ligands.[61] Their goal was to study the distance dependency of magnetic effects with respect to protons on a ligand. Ligands with pyridine moieties for zinc(II) coordination and protons with varying distances to the por-

phyrin sheet **130** in the form of 1,3-bis(pyridin-3-ylethynyl)benzene (**200**), 4,4′-bipyridine (**197**), 1,4-di(pyridin-4-yl)benzene (**198**) and 4,4′-di(pyridin-4-yl)-1,1′-biphenyl (**199**) were employed[62] (Scheme 39). All three linear pyridine ligands appeared to form 2:4 complexes with the porphyrin sheet, while the bent ligand **200** was found to complex the porphyrin sheet in a 1:2 stoichiometry. The proton NMR data of the bound linear ligands, showing a simple signal pattern, led Osuka and co-workers to the conclusion that these ligands underwent free rotation within the complex. On comparing the chemical shifts from the proton NMR spectra of the unbound and bound ligands, two trends became apparent: first, the deshielding influences of the porphyrin sheet decreases with increasing ligand length, and second, the order of magnitude in chemical shift was found to be: $H^\beta > H^\gamma > H^\delta > H^\alpha$. Due to free rotation, the examined protons experience only an average of the ring-current strength above the porphyrin subunit. The non-linear ligand, 1,3-bis(pyridin-3-ylethynyl)benzene (**200**), was studied because its protons are positioned at different heights above the porphyrin subunit and the COT core. When comparing the chemical shifts of the protons above the porphyrin subunit, only H^f is far enough away from the COT core to experience a net diatropic ring current. By contrast, H^g resides closer to the COT core and is influenced distinctly stronger by the paratropic ring current. The induced magnetic effect changes from an upfield to downfield shift with increasing distance to the porphyrin plane, as seen in the difference in the downfield shift observed for the signals of H^f to H^e. Proton H^c resided directly on top of the COT core and experienced the strongest para-

tropic ring current. The magnetic effect of the COT core was also found to decrease with increasing distance of the nuclei, based on the chemical shifts of protons H^c, H^b and H^a. NICS calculations on ghost atoms placed at varying distances above the COT core agreed with this observation, giving an exponential relationship between distance and NICS value. NICS values were also calculated for varying points in the plane and above the plane of the tetramer, as well as in between two sheets of the tetramer. The NICS values above the zinc atoms were found to be negative (diatropic magnetic effect) for small distances. Increasing the distance to the porphyrin sheet, the NICS value would grow rapidly to positive values (paratropic magnetic effect) and slowly decrease again. These results agree well with the experimental data. In contrast, the NICS values calculated in between two porphyrin sheets do not account well for the experimental data, presumably due to dynamic motion and deformation processes of the complexes.

In 2011, Minaev, Baryshnikov and Minaeva[63] performed a DFT study [with optimization at the B3LYP/6-31G(d) level] on many of the tetraoxa[8]circulenes synthesized by Christensen and Pittelkow in 2010, together with one of Rathore's tetraoxa[8]circulenes from 2004. The calculations reproduced reasonably the UV/Vis and IR spectra of these compounds. The following year, Pittelkow collaborated with these authors to publish a DFT study on the benzoquinone and naphthoquinone circulenes, arriving at good agreement between simulation and experiment for the vibrational modes of these compounds.[64] In further theoretical studies, in collaboration with Salcedo and Pittelkow, the local aromatic and antiaromatic character of different tetraoxa[8]circulene systems was investigated by NICS indices.[65] The NICS(0) and NICS(1) values presented in Figure 12 were calculated by the B3LYP/6-311+G(d,p) method.

The positive NICS(0) values of the COT cores of the tetraoxa[8]circulenes ranged from 6.55 to 9.23, suggesting antiaromaticity. By annulating benzenes, the antiaromatic character seems to be decreased. Attaching bicycloalkanes conversely led to larger values. Overall, the COT cores exhibit relatively small NICS values when compared to the standard D_{4h} COT with an NICS(0) value of 30.1 at the B3LYP/6-31 G* level. The naphthalene and benzene moieties in the tetraoxa[8]circulene feature NICS values comparable to those of benzene and naphthalene themselves. A significant difference was observed when comparing the NICS values of furan with those of the furan moieties within the circulenes. The authors suggested this was due to conjugation of the furan ring with benzenes on each side, delocalizing the furan π-electron system into the neighboring rings.[65]

Nenajdenko, Antipin and co-workers published the NICS(1) values of sulflower in 2008.[66] The COT core of this compound gave a positive NICS(1) value of 2.4, indicating weak magnetic antiaromaticity. The negative value (−7.1) of
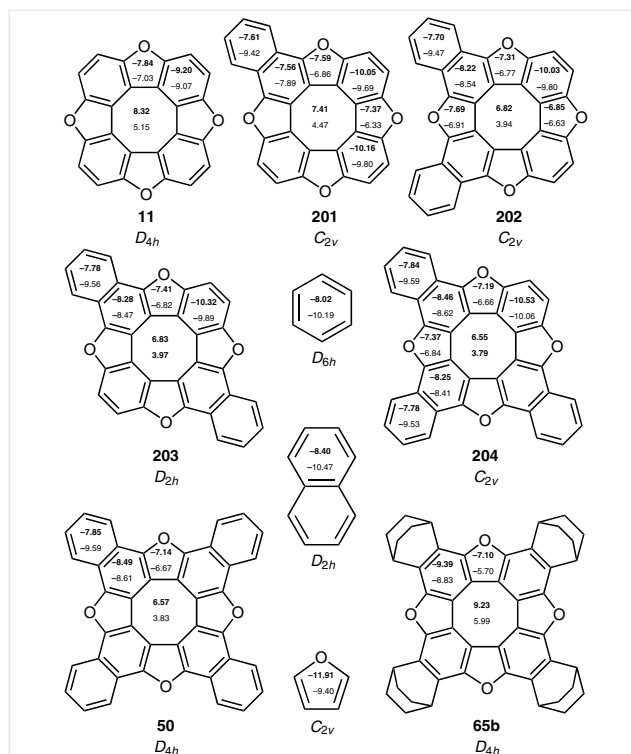
Figure 12 NICS values of differently annulated tetraoxa[8]circulenes. NICS(0) values are presented in bold font and NICS(1) in regular font[65]

the thiophene subunits hints at an aromatic π-system, with somewhat reduced aromaticity compared to thiophene itself (−10.2).

To address the overall magnetic current in hetero[8]circulenes, NICS and gauge-including magnetically induced currents (GIMIC) calculations (at the B3LYP/TZVP level) were conducted by Minaev and co-workers in 2014.[67] The GIMIC calculations allow for an estimation of the overall ring current strengths where positive values indicate overall aromatic, and negative values indicate overall antiaromatic ring current. Benzene, as a typical aromatic compound, was calculated to have a total ring current of +11.8 nA T^{-1} while antiaromatic cyclobutadiene featured a value of −19.9 nA T^{-1}. Non-aromatic cyclohexane was calculated to have a total ring current of 0.2 nA T^{-1}. The calculated global ring current strengths (I_{tot}) of hetero[8]circulenes were found to be either slightly antiaromatic (negative I_{tot}) or non-aromatic (very small I_{tot} values around zero). An overall non-aromatic system was indicated by the similar size of the NICS values of the benzene, furan, and pyrrole subunits and the COT core, which might cancel out. It has been determined that the hetero[8]circulenes with one to four nitrogen atoms experience a decrease in the numerical value of the total ring current strength with an increasing amount of nitrogen atoms (1 × N with I_{tot} = −3.1 nA T^{-1} and 4 × N with I_{tot} = −0.5 nA T^{-1}). Azatrioxa[8]circulene displays

a higher total ring current than tetraoxa[8]circulene (I_{tot} = –2.1 nA T^{-1}). In conclusion, tetraoxa-, azatrioxa-, and diaza-dioxa[8]circulene can be considered to be overall slightly antiaromatic according to GIMIC calculations. One compound, the tetraselenotetrathia[8]circulene, featured a small positive total ring current of 0.6 nA T^{-1}, making it non-aromatic. Other heterocyclic [8]circulenes also exhibited non-aromaticity, but with small negative total ring currents, for example, triazamonooxa[8]circulene (–0.6 nA T^{-1}), tetraaza[8]circulene (–0.5 nA T^{-1}) and sulflower (–0.2 nA T^{-1}).[67] In a recent review, Baryshnikov, Minaev and Minaeva presented experimental and theoretical data on the electronic structure, aromaticity and spectra of hetero[8]circulenes.[68]

In our recent work on azatrioxa[8]circulenes[6b,34] and diazadioxa[8]circulenes,[6c] we addressed the question of aromaticity and antiaromaticity in the benzene, furan and COT subunits via geometry optimizations and NICS calculations. Geometries were obtained in B3LYP/6-31+G(d) calculations and employed in NICS(0) and NICS(1) calculations at the B3LYP/6-311+G(d,p) level of theory. The studied molecules in their oxidized and reduced forms are presented in Figure 13, along with the respective NICS(0) and NICS(1) values. The positive NICS values concerning the planar COT core in the neutral forms of tetraoxa- **11**, azatrioxa- **12** and diazadioxa[8]circulene **205** are almost identical and suggest a magnetic antiaromatic character. The benzene, furan and pyrrole rings exhibit aromatic character with negative NICS values, in accordance with our experimental data. Curiously, the NICS values of the doubly oxidized tetraoxa[8]circulene **11²⁺** indicate a weakening of the antiaromaticity of the COT core. Azatrioxa[8]circulene **12²⁺** experiences significantly smaller NICS(1) values, while the NICS(0) values are slightly larger; diazadioxa[8]circulene **205²⁺** features significantly larger NICS(0) and NICS(1) values. In the case of the doubly negative charged species, the large negative values hint at an aromatic COT core. The bond length fluctuations were found to be significantly lower for the aromatic doubly reduced species. It could be argued, that the observed ring-current effect in the COT core arises solely from the combined ring-current effects of the linked benzenes.[6b] However, NICS calculations of a ghost atom placed next to a benzene or next to two benzenes, with distances identical to those in tetraoxa[8]circulene **11**, revealed values of about 1 and 2, respectively. A dummy atom surrounded by four equiplanar benzenes should yield a value of up to 4, in contrast to the values above 8 calculated for the neutral hetero[8]circulenes displayed in Figure 13.
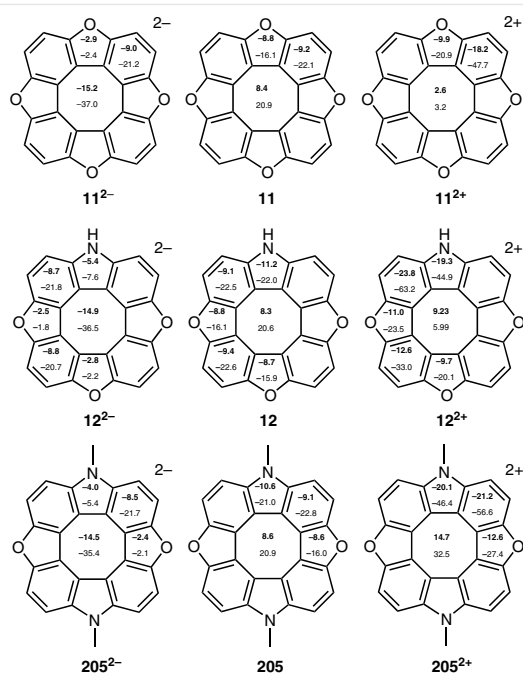
Figure 13 NICS values of tetraoxa-, azatrioxa- and diazadioxa[8]circulenes, including their doubly reduced and doubly oxidized derivatives. NICS(0) values are presented in bold font and NICS(1) values in regular font[6b,c]

Nishinaga and co-workers recently published a study on the aromaticity and antiaromaticity of the compounds presented in Figure 14 (the syntheses of these compounds are described in Scheme 33).[49] Their study highlighted different combinations of *ortho*-annulated aromatic compounds in order to obtain COT structures of varying geometries (see Figure 4). Optimizations at the B3LYP/6-31G(d,p) level determined the most stable conformer of dithiophene COT **161** to be almost completely planar (C_{2v} structure), in contrast to the slightly bent structures of tetrathiophene COT **151** and significantly bent fluorene COT **207**. The COT core of **161** exhibited very small deviations concerning the inner angles in the optimized structures (133.2° to 136.8°) compared to the ideal D_{4h} octagon with angles of 135°. Compound **206**, having a deformed COT core, experienced larger deviations (124.0° to 143.5°). The simulated X-ray data corresponded well with the experimental values. Interestingly, the experimental data of dithiophene-COT **161** showed two crystallographically independent conformers, one slightly bent (shorter intermolecular C–H contacts caused by crystal packing forces) and the other planar. DFT calculations in the form of NICS values, concerning the dithiophene compound **161**, showed higher antiaromaticity (80% of D_{4h} COT) than tetrathiophene compound **151** (70% of D_{4h} COT). It was assumed that the difference in antiaromaticity was due to the higher annulation of **151** with aromatic molecules, reducing the overall antiaromaticity of the COT core. Moreover, the magnetic antiaromatic character and planarity of

the COT, demonstrated by the NICS values, decreased in the following order: dithiophene-COT **161** > tetrathiophene-COT **151** > phenylene-COT **206** > fluorene-COT **207**. Another indication of the antiaromatic character would be a narrow HOMO–LUMO gap. However, the increased antiaromatic character of dithiophene **161** compared to tetrathiophene **151** did not result in a smaller HOMO–LUMO gap, as UV/Vis spectra and CV studies exhibited similar values for both compounds. Phenylene-COT **206** and fluorene-COT **207** were found, by UV/Vis spectroscopy and cyclic voltammetry, to have a larger HOMO–LUMO gap, consistent with the calculated lower antiaromaticity. To determine the magnetic ring-current effects of the COT core experimentally, Nishinaga and co-workers recorded proton NMR spectra and found upfield shifts for the signals due to protons H^a and H^b, compared to those in cyclooctatriene **160** (Figure 14). The differences in the upfield shifts appeared to concur with the obtained NICS values, as protons H^a and H^b of dithiophene COT **161** exhibited the highest upfield shifts and those protons of fluorene-COT **207** the lowest. The diatropic ring current of the thiophene and benzene groups appeared to weaken the influence of the magnetic ring current on proton H^a. The recorded crystal structures exhibited short distances between the thiophene protons and the COT unit between neighboring molecules. For this reason, solid state NMR analysis was conducted by Nishinaga et al. Their calculations predicted a large downfield shift of around 3.2–3.5 ppm. The actual recorded solid state NMR data, however, revealed a signal shift of only 0.6 ppm.[45,49]
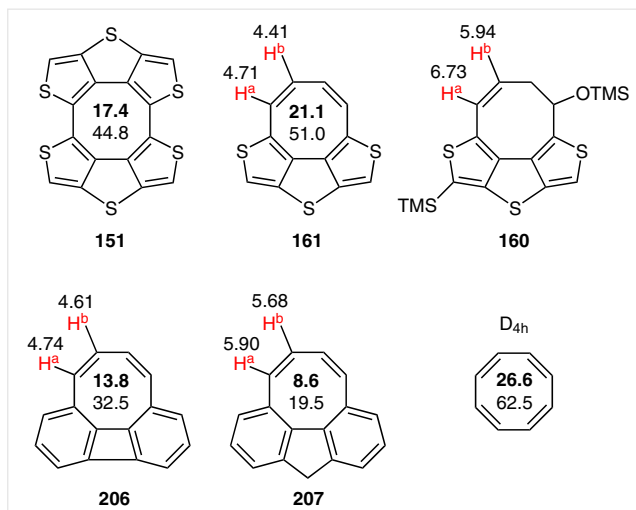
Figure 14 NICS(0) and NICS(1) values and experimental chemical shifts of the COT protons obtained by Iyoda and Nishinaga[45,49]

Wong's tetrathia- and tetraselena[8]circulenes, published in 2014, were also subjected to NICS calculations at the B3LYP/6-311+G(d,p) level of theory.[50] The investigated compounds along with their corresponding NICS(0) values

are presented in Figure 15. Similar to the aza- and oxa[8]circulenes, the benzene, thiophene and selenophene rings were aromatic, as indicated by the obtained negative NICS values (–5.9 to –10.3). The central COT in tetrathia-**133** and tetraselena[8]circulene **134** exhibited positive NICS values of 7.0 and 8.2, respectively, implying an antiaromatic character. The small value of 2.3 in the central COT of tetraphenylene **131** most likely arose from the magnetic effect of the four benzene moieties surrounding it. It was further observed that the four compounds with only two sulfur (**174**, **208**) or two selena bridges (**176**, **209**), in general, feature lowered NICS values.
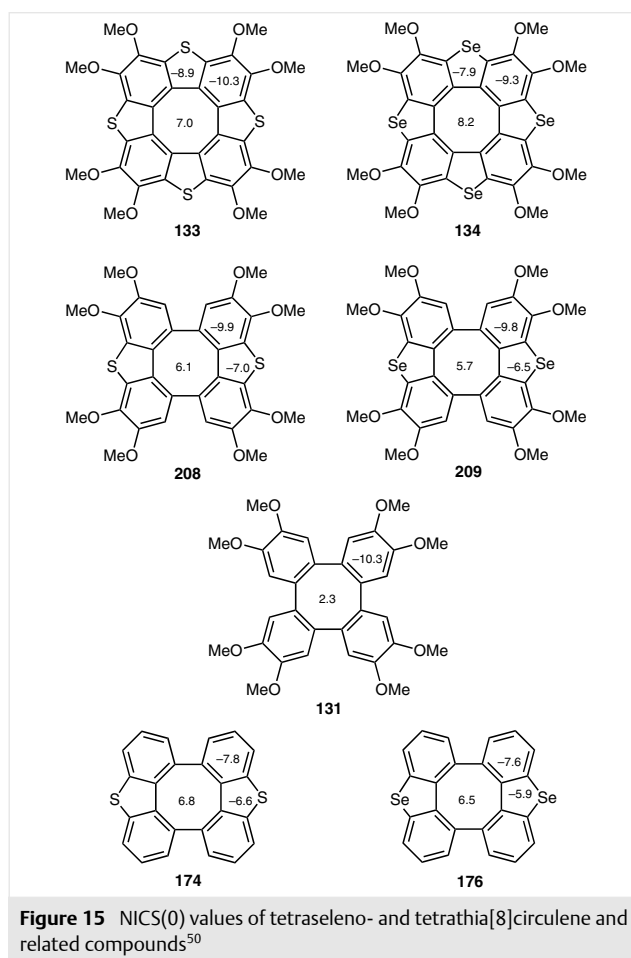
Figure 15 NICS(0) values of tetraseleno- and tetrathia[8]circulene and related compounds[50]

Nguyen et al. recently investigated different hetero[8]circulenes with oxygen, nitrogen, selenium and sulfur bridges by DFT calculations. They carried out geometry optimizations at the B3LYP/6-31G(d,p) level of theory. These optimizations displayed a bond-length increase of the order C–O ~ C–N < C–S < C–Se. As a result, the tetraoxa[8]circulene, tetraaza[8]circulene and tetrathia[8]circulene feature planar structures, while tetraseleno[8]circulene was predicted to be slightly bent, as confirmed by Wong et al. in

2015. The calculated NICS(0) values of the COT core decrease with the increasing size of the heteroatom of the annulated heterocycles (tetraoxa: 8.4 > tetraaza: 8.0 > tetrathia: 6.7 > tetraseleno: 4.1). The same trend was observed for the NICS(1) values, with the exception that the selenium compounds exhibited the largest values. Overall, the calculations indicated a magnetically antiaromatic COT core and aromatic annulated five- and six-membered cycles, which is in accordance with many previous studies performed on hetero[8]circulenes.[6b,c,34,44,45,50] The simulated UV/Vis spectra corresponded well with the previous studies.

9 Conclusion and Outlook

In this account, we have presented an introduction to the synthesis of [n]circulenes, hetero[8]circulenes and related systems. The geometry model that we have proposed expands on Dopper and Wynberg's model and is inspired by Erdtman and Högberg's work on quinones and tetraoxa[8]circulenes. We have presented our work on azatrioxa[8]circulenes and diazadioxa[8]circulenes, and have described the influence of previous studies and our recent work regarding tetraoxa[8]circulene on the synthetic approach toward our nitrogen-containing hetero[8]circulenes. We have also described the syntheses of other hetero[8]circulenes and related systems. An important application of this class of compounds is in the investigation of aromaticity and antiaromaticity. In the final section, we outlined different definitions of these concepts and compared the calculated and experimental data concerning the field of aromaticity and antiaromaticity. Other major applications of hetero[8]circulenes, for example as organic light-emitting diodes or in DNA intercalation, highlight the importance of undertaking further investigations.

Acknowledgment

References

(1) (a) Christoph, H.; Grunenberg, J.; Hopf, H.; Dix, I.; Jones, P. G.; Scholtissek, M.; Maier, G. *Chem. Eur. J.* **2008**, *14*, 5604. (b) Gholami, M.; Tykwinski, R. R. *Chem. Rev.* **2006**, *106*, 4997. (c) Hopf, H. *Angew. Chem. Int. Ed.* **2012**, *51*, 11945.

(2) Kroto, H. W.; Heath, J. R.; O'Brien, S. C.; Curl, R. F.; Smalley, R. E. *Nature* **1985**, *318*, 162.

(3) Dopper, J. H.; Wynberg, H. *J. Org. Chem.* **1975**, *40*, 1957.

(4) Högberg, H.-E. *Cyclo-Oligomerization of Quinones, Ph.D. Thesis*; Royal Institute of Technology: Sweden, **1973**.

(5) (a) Kanakaraju, R.; Kolandaivel, P. *Int. J. Mol. Sci.* **2002**, *3*, 777. (b) Kwiatkowski, J. S.; Leszczynski, J.; Teca, I. *J. Mol. Struct.* **1997**, *437*, 451. (c) O'Sullivan, P. S.; Hameka, H. F. *Chem. Phys. Lett.* **1969**, *4*, 123.

(6) (a) Mejlsøe, S. L.; Christensen, J. B. *J. Heterocycl. Chem.* **2014**, *51*, 1051. (b) Nielsen, C. B.; Brock-Nannestad, T.; Hammershøj, P.; Reenberg, T. K.; Schau-Magnussen, M.; Trpcevski, D.; Hensel, T.; Salcedo, R.; Baryshnikov, G. V.; Minaev, B. F.; Pittelkow, M. *Chem. Eur. J.* **2013**, *19*, 3898. (c) Hensel, T.; Trpcevski, D.; Lind, C.; Grosjean, R.; Hammershøj, P.; Nielsen, C. B.; Brock-Nannestad, T.; Nielsen, B. E.; Schau-Magnussen, M.; Minaev, B.; Baryshnikov, G. V.; Pittelkow, M. *Chem. Eur. J.* **2013**, *19*, 17097. (d) Feng, C.-N.; Kuo, M.-Y.; Wu, Y.-T. *Angew. Chem. Int. Ed.* **2013**, *52*, 7791. (e) Kumar, B.; King, B. T. *J. Org. Chem.* **2012**, *77*, 10617. (f) Dadvand, A.; Cicoira, F.; Chernichenko, K. Y.; Balenkova, E. S.; Osuna, R. M.; Rosei, F.; Nenajdenko, V. G.; Perepichka, D. F. *Chem. Commun.* **2008**, 5354. (g) Nakamura, Y.; Aratani, N.; Shinokubo, H.; Takagi, A.; Kawai, T.; Matsumoto, T.; Yoon, Z. S.; Kim, D. Y.; Ahn, T. K.; Kim, D.; Muranaka, A.; Kobayashi, N.; Osuka, A. *J. Am. Chem. Soc.* **2006**, *128*, 4119. (h) Peng, H.-Y.; Lam, C.-K.; Mak, T. C. W.; Cai, Z.; Ma, W.-T.; Li, Y.-X.; Wong, H. N. C. *J. Am. Chem. Soc.* **2005**, *127*, 9603. (i) Sakurai, H.; Daiko, T.; Hirao, T. *Science* **2003**, *301*, 1878. (j) Scott, L. T.; Hashemi, M. M.; Meyer, D. T.; Warren, H. B. *J. Am. Chem. Soc.* **1991**, *113*, 7082. (k) Yamamoto, K.; Harada, T.; Nakazaki, M.; Naka, T.; Kai, Y.; Harada, S.; Kasai, N. *J. Am. Chem. Soc.* **1983**, *105*, 7171. (l) Hellwinkel, D.; Reiff, G. *Angew. Chem. Int. Ed.* **1970**, *9*, 527.

(7) Bharat, ; Bhola, R.; Bally, T.; Valente, A.; Cyrański, M. K.; Dobrzycki, Ł.; Spain, S. M.; Rempała, P.; Chin, M. R.; King, B. T. *Angew. Chem. Int. Ed.* **2010**, *49*, 399.

(8) Barth, W. E.; Lawton, R. G. *J. Am. Chem. Soc.* **1966**, *88*, 380.

(9) Wu, Y.-T.; Siegel, J. S. *Chem. Rev.* **2006**, *106*, 4843.

(10) Scholl, R.; Meyer, K. *Ber. Dtsch. Chem. Ges.* **1932**, *65*, 902.

(11) Novoselov, K. S.; Falko, V. I.; Colombo, L.; Gellert, P. R.; Schwab, M. G.; Kim, K. *Nature* **2012**, *490*, 192.

(12) Shen, H.-C.; Tang, J.-M.; Chang, H.-K.; Yang, C.-W.; Liu, R.-S. *J. Org. Chem.* **2005**, *70*, 10113.

(13) Anthony, J. W.; Bideaux, R. A.; Bladh, K. W.; Nichols, M. C. *Handbook of Mineralogy - Volume V: Borates, Carbonates, Sulfates*; Mineral Data Publishing: Tucson, **1990**.

(14) Shen, M.; Ignatyev, I. S.; Xie, Y.; Schaefer, H. F. *J. Phys. Chem.* **1993**, *97*, 3212.

(15) Yamamoto, K.; Sonobe, H.; Matsubara, H.; Sato, M.; Okamoto, S.; Kitaura, K. *Angew. Chem., Int. Ed. Engl.* **1996**, *35*, 69.

(16) (a) Miller, R. W.; Duncan, A. K.; Schneebeli, S. T.; Gray, D. L.; Whalley, A. C. *Chem. Eur. J.* **2014**, *20*, 3705. (b) Sakamoto, Y.; Suzuki, T. *J. Am. Chem. Soc.* **2013**, *135*, 14074.

(17) Högberg, H. E. *Acta Chem. Scand.* **1973**, *27*, 2559.

(18) von Knapp, H.; Schultz, G. *Liebigs Ann. Chem.* **1881**, *210*, 164.

(19) Liebermann, C. *Chem. Ber.* **1885**, *18*, 966.

(20) (a) Erdtman, H. G. H. *Proc. R. Soc. London Ser. A* **1933**, *143*, 177. (b) Erdtman, H. G. H. *Proc. R. Soc. London Ser. A* **1933**, *143*, 191. (c) Erdtman, H. G. H. *Proc. R. Soc. London Ser. A* **1933**, *143*, 223. (d) Erdtman, H. G. H. *Proc. R. Soc. London Ser. A* **1933**, *143*, 228.

(21) Pummerer, R.; Frankfurter, F. *Chem. Ber.* **1914**, *47*, 1472.

(22) Erdtman, H.; Högberg, H. E. *Chem. Commun.* **1968**, 773.

(23) Hewgill, F. R.; Kennedy, B. R. *J. Chem. Soc. C* **1966**, 362.

(24) (a) Erdtman, H.; Högberg, H. E. *Tetrahedron Lett.* **1970**, 3389. (b) Högberg, H. E. *Acta Chem. Scand.* **1972**, *26*, 309.

(25) (a) Högberg, H. E. *Acta Chem. Scand.* **1972**, *26*, 2752. (b) Högberg, H. E. *Acta Chem. Scand.* **1973**, *27*, 2591.

(26) Erdtman, H. G. H.; Högberg, H. E. *Heterocycles* **1977**, *8*, 171.

(27) Erdtman, H.; Högberg, H.-E. *Tetrahedron* **1979**, *35*, 535.

(28) Eskildsen, J.; Reenberg, T.; Christensen, J. B. *Eur. J. Org. Chem.* **2000**, 1637.

(29) Hashmat Ali, M.; Niedbalski, M.; Bohnert, G.; Bryant, D. *Synth. Commun.* **2006**, *36*, 1751.

(30) Rathore, R.; Abdelwahed, S. H. *Tetrahedron Lett.* **2004**, *45*, 5267.

(31) Nielsen, C. B.; Brock-Nannestad, T.; Reenberg, T. K.; Hammershoj, P.; Christensen, J. B.; Stouwdam, J. W.; Pittelkow, M. *Chem. Eur. J.* **2010**, *16*, 13030.

(32) Brock-Nannestad, T.; Nielsen, C. B.; Schau-Magnussen, M.; Hammershoj, P.; Reenberg, T. K.; Petersen, A. B.; Trpcevski, D.; Pittelkow, M. *Eur. J. Org. Chem.* **2011**, 6320.

(33) Brooks, P. R.; Wirtz, M. C.; Vetelino, M. G.; Rescek, D. M.; Woodworth, G. F.; Morgan, B. P.; Coe, J. W. *J. Org. Chem.* **1999**, *64*, 9719.

(34) Plesner, M.; Hensel, T.; Nielsen, B. E.; Kamounah, F. S.; Brock-Nannestad, T.; Nielsen, C. B.; Tortzen, C. G.; Hammerich, O.; Pittelkow, M. *Org. Biomol. Chem.* **2015**, *13*, 5937.

(35) Lessene, G.; Feldman, K. S. *Oxidative Aryl-Coupling Reactions in Synthesis*, In *Modern Arene Chemistry*; Astruc, D., Ed.; Wiley-VCH: Weinheim, **2004**, 479–538.

(36) Botman, P. N. M.; Postma, M.; Fraanje, J.; Goubitz, K.; Schenk, H.; van Maarseveen, J. H.; Hiemstra, H. *Eur. J. Org. Chem.* **2002**, 1952.

(37) Rogers, C. U.; Corson, B. B. *J. Am. Chem. Soc.* **1947**, *69*, 2910.

(38) Liu, L.; Carroll, P. J.; Kozlowski, M. C. *Org. Lett.* **2015**, *17*, 508.

(39) Chernichenko, K. Y.; Sumerin, V. V.; Shpanchenko, R. V.; Balenkova, E. S.; Nenajdenko, V. G. *Angew. Chem. Int. Ed.* **2006**, *45*, 7367.

(40) Perepichka, I. F.; Perepichka, D. F.; Meng, H.; Wudl, F. *Adv. Mater.* **2005**, *17*, 2281.

(41) Sun, Y.; Liu, Y.; Zhu, D. *J. Mater. Chem.* **2005**, *15*, 53.

(42) Barbarella, G.; Melucci, M.; Sotgiu, G. *Adv. Mater.* **2005**, *17*, 1581.

(43) Nakamura, Y.; Aratani, N.; Furukawa, K.; Osuka, A. *Tetrahedron* **2008**, *64*, 11433.

(44) Xiong, X.; Deng, C.-L.; Minaev, B. F.; Baryshnikov, G. V.; Peng, X.-S.; Wong, H. N. C. *Chem. Asian J.* **2015**, *10*, 969.

(45) Ohmae, T.; Nishinaga, T.; Wu, M.; Iyoda, M. *J. Am. Chem. Soc.* **2010**, *132*, 1066.

(46) Chen, F.; Hong, Y. S.; Shimizu, S.; Kim, D.; Tanaka, T.; Osuka, A. *Angew. Chem. Int. Ed.* **2015**, *54*, 10639.

(47) (a) Reiff, G. *Diplomarbeit*; University of Heidelberg: Germany, **1969**. (b) Hellwinkel, D.; Reiff, G.; Nykodym, V. *Liebigs Ann. Chem.* **1977**, 1013.

(48) Iyoda, M.; Miura, M.; Sasaki, S.; Kabir, S. M. H.; Kuwatani, Y.; Yoshida, M. *Tetrahedron Lett.* **1997**, *38*, 4581.

(49) Aita, K.; Ohmae, T.; Takase, M.; Nomura, K.; Kimura, H.; Nishinaga, T. *Org. Lett.* **2013**, *15*, 3522.

(50) Xiong, X.-D.; Deng, C.-L.; Peng, X.-S.; Miao, Q.; Wong, H. N. C. *Org. Lett.* **2014**, *16*, 3252.

(51) Baker, W.; Barton, J. W.; McOmie, J. F. W. *J. Chem. Soc.* **1958**, 2658.

(52) Kabir, S. M. H.; Iyoda, M. *Synthesis* **2000**, 1839.

(53) Nobusue, S.; Miyoshi, H.; Shimizu, A.; Hisaki, I.; Fukuda, K.; Nakano, M.; Tobe, Y. *Angew. Chem. Int. Ed.* **2015**, *54*, 2090.

(54) (a) De Proft, F.; Geerlings, P. *Chem. Rev.* **2001**, *101*, 1451. (b) Zhou, Z.; Parr, R. G. *J. Am. Chem. Soc.* **1989**, *111*, 7371.

(55) Ruiz-Morales, Y. *J. Phys. Chem. A* **2002**, *106*, 11283.

(56) Rague von Schleyer, P.; Jiao, H. *Pure Appl. Chem.* **1996**, *68*, 209.

(57) (a) Carey, F. A.; Sundberg, R. J. *Advanced Organic Chemistry, Part A: Structure and Mechanisms*, 5th ed.; Springer: New York, **2007**, 713–770. (b) Rauk, A. *Aromatic Compounds*, In *Orbital Interaction Theory of Organic Chemistry*, 2nd ed.; John Wiley & Sons: New York, **2002**, 150.

(58) Komatsu, K.; Nishinaga, T.; Aonuma, S.; Hirosawa, C.; Takeuchi, K.-i.; Lindner, H. J.; Richter, J. *Tetrahedron Lett.* **1991**, *32*, 6767.

(59) Komatsu, K.; Aonuma, S.; Jinbu, Y.; Tsuji, R.; Hirosawa, C.; Takeuchi, K. *J. Org. Chem.* **1991**, *56*, 195.

(60) Matsuura, A.; Komatsu, K. *J. Am. Chem. Soc.* **2001**, *123*, 1768.

(61) Nakamura, Y.; Aratani, N.; Osuka, A. *Chem. Asian J.* **2007**, *2*, 860.

(62) (a) Schultheiss, N.; Ellsworth, J. M.; Bosch, E.; Barnes, C. L. *Eur. J. Inorg. Chem.* **2005**, 45. (b) Biradha, K.; Fujita, M. *J. Chem. Soc., Dalton Trans.* **2000**, 3805. (c) Biradha, K.; Hongo, Y.; Fujita, M. *Angew. Chem. Int. Ed.* **2000**, *39*, 3843.

(63) Minaev, B. F.; Baryshnikov, G. V.; Minaeva, V. A. *Comput. Theor. Chem.* **2011**, *972*, 68.

(64) Minaeva, V. A.; Minaev, B. F.; Baryshnikov, G. V.; Agren, H.; Pittelkow, M. *Vib. Spectrosc.* **2012**, *61*, 156.

(65) Baryshnikov, G.; Minaev, B.; Pittelkow, M.; Nielsen, C.; Salcedo, R. *J. Mol. Model.* **2013**, *19*, 847.

(66) Bukalov, S. S.; Leites, L. A.; Lyssenko, K. A.; Aysin, R. R.; Korlyukov, A. A.; Zubavichus, J. V.; Chernichenko, K. Y.; Balenkova, E. S.; Nenajdenko, V. G.; Antipin, M. Y. *J. Phys. Chem. A* **2008**, *112*, 10949.

(67) Baryshnikov, G. V.; Valiev, R. R.; Karaush, N. N.; Minaev, B. F. *PCCP* **2014**, *16*, 15367.

(68) Baryshnikov, G. V.; Minaev, B. F.; Minaeva, V. A. *Russ. Chem. Rev.* **2015**, *84*, 455.